



NAVAL POSTGRADUATE SCHOOL

MONTEREY, CALIFORNIA

THESIS

WAVEFORM DESIGN COMPENSATION FOR MOVING EXTENDED TARGETS

by

Emmanouil Mourtzakis

June 2013

Thesis Advisor:
Second Reader:

Ric Romero
Tri Ha

Approved for public release; distribution is unlimited

THIS PAGE INTENTIONALLY LEFT BLANK

REPORT DOCUMENTATION PAGE			<i>Form Approved OMB No. 0704-0188</i>	
Public reporting burden for this collection of information is estimated to average 1 hour per response, including the time for reviewing instruction, searching existing data sources, gathering and maintaining the data needed, and completing and reviewing the collection of information. Send comments regarding this burden estimate or any other aspect of this collection of information, including suggestions for reducing this burden, to Washington headquarters Services, Directorate for Information Operations and Reports, 1215 Jefferson Davis Highway, Suite 1204, Arlington, VA 22202-4302, and to the Office of Management and Budget, Paperwork Reduction Project (0704-0188) Washington DC 20503.				
1. AGENCY USE ONLY (Leave blank)		2. REPORT DATE June 2013	3. REPORT TYPE AND DATES COVERED Master's Thesis	
4. TITLE AND SUBTITLE WAVEFORM DESIGN COMPENSATION FOR MOVING EXTENDED TARGETS			5. FUNDING NUMBERS	
6. AUTHOR(S) Emmanouil Mourtzakis				
7. PERFORMING ORGANIZATION NAME(S) AND ADDRESS(ES) Naval Postgraduate School Monterey, CA 93943-5000			8. PERFORMING ORGANIZATION REPORT NUMBER	
9. SPONSORING /MONITORING AGENCY NAME(S) AND ADDRESS(ES) N/A			10. SPONSORING/MONITORING AGENCY REPORT NUMBER	
11. SUPPLEMENTARY NOTES The views expressed in this thesis are those of the author and do not reflect the official policy or position of the Department of Defense or the U.S. Government. IRB Protocol number ____N/A____.				
12a. DISTRIBUTION / AVAILABILITY STATEMENT Approved for public release; distribution is unlimited			12b. DISTRIBUTION CODE	
13. ABSTRACT (maximum 200 words) <p>The Cognitive Radar (CR) is a new field for radar research. Its basic characteristics are introduced in this thesis. Two specific types of waveforms are used in this research; wideband and an adaptive waveform called probability weighted energy (PWE) waveform. This thesis also illustrates a comparison of two approaches to using a target recognition CR system. The first approach is to set a specific probability threshold but without limiting the number of transmissions. In contrast, the second approach is to set a specific number of transmissions. Moreover, waveform design due to moving target and a static target recognition CR system using wideband waveform and PWE waveform is presented. For a target whose extent changes with motion, a CR system must compensate the waveforms in order to mitigate the effect on performance.</p>				
14. SUBJECT TERMS Cognitive Radar (CR), Probability Weighted Energy (PWE) waveform, Probability of Correct Decision (P_{cd}), Compensated Wideband waveform, Compensated PWE waveform, Extended target			15. NUMBER OF PAGES 93	
			16. PRICE CODE	
17. SECURITY CLASSIFICATION OF REPORT Unclassified	18. SECURITY CLASSIFICATION OF THIS PAGE Unclassified	19. SECURITY CLASSIFICATION OF ABSTRACT Unclassified	20. LIMITATION OF ABSTRACT UU	

THIS PAGE INTENTIONALLY LEFT BLANK

Approved for public release; distribution is unlimited

**WAVEFORM DESIGN COMPENSATION FOR MOVING EXTENDED
TARGETS**

Emmanouil Mourtzakis
Lieutenant, Hellenic Navy
B.S., Hellenic Naval Academy, 2002
M.S., University of Piraeus, 2009

Submitted in partial fulfillment of the
requirements for the degree of

MASTER OF SCIENCE IN ELECTRICAL ENGINEERING

from the

**NAVAL POSTGRADUATE SCHOOL
June 2013**

Author: Emmanouil Mourtzakis

Approved by: Ric Romero
Thesis Advisor

Tri Ha
Second Reader

R. Clark Robertson
Chair, Department of Electrical and Computer Engineering

THIS PAGE INTENTIONALLY LEFT BLANK

ABSTRACT

The Cognitive Radar (CR) is a new field for radar research. Its basic characteristics are introduced in this thesis. Two specific types of waveforms are used in this research; wideband and an adaptive waveform called probability weighted energy (PWE) waveform. This thesis also illustrates a comparison of two approaches to using a target recognition CR system. The first approach is to set a specific probability threshold but without limiting the number of transmissions. In contrast, the second approach is to set a specific number of transmissions. Moreover, waveform design due to moving target and a static target recognition CR system using wideband waveform and PWE waveform is presented. For a target whose extent changes with motion, a CR system must compensate the waveforms in order to mitigate the effect on performance.

THIS PAGE INTENTIONALLY LEFT BLANK

TABLE OF CONTENTS

I.	INTRODUCTION.....	1
A.	BACKGROUND	1
B.	THESIS OBJECTIVE	1
C.	THESIS OUTLINE.....	2
D.	APPROACH.....	3
II.	COGNITIVE RADAR AND PROBABILITY WEIGHTED ENERGY (PWE) WAVEFORM	5
A.	COGNITIVE RADAR CHARACTERISTICS.....	5
1.	Cognitive Signal Processing Cycle.....	5
2.	Radar-Scene Analysis	5
B.	PROBABILIY WEIGHTED ENERGY (PWE) WAVEFORM.....	6
C.	PWE TECHNIQUE MATHEMATICAL BACKGROUND	6
1.	One Transmission Using the PWE Waveform.....	8
2.	K Number of Transmissions Using the PWE Waveform	11
D.	CHAPTER SUMMARY.....	13
III.	CLOSED-LOOP RADAR SYSTEM: A CASE STUDY OF TWO TECHNIQUES.....	15
A.	INTRODUCTION.....	15
B.	PROBABILITY THRESHOLD AND AVERAGE NUMBER OF TRANSMISSIONS (ANTR)	15
C.	MEAN AND APPROXIMATE NUMBER OF TRANSMISSION GIVEN CORRECT DECISION.....	17
D.	FIXED NUMBER OF TRANSMISSIONS.....	23
E.	AVERAGE CORRECT TERMINAL PROBABILITY (ACTP)	25
1.	Introduction.....	25
2.	ACTP for WI Waveform.....	26
3.	ACTP for PWE Waveform	27
F.	P_{cd} AND ACTP FOR WIDEBAND WAVEFORM	30
G.	P_{cd} AND ACTP FOR PWE WAVEFORM.....	34
H.	CHAPTER SUMMARY.....	39
IV.	PROBABILITY OF CORRECT DECISION (P_{cd}) FOR MOVING EXTENDED TARGETS	43
A.	INTRODUCTION.....	43
B.	CONCEPT APPROACH	43
C.	EXTENSION TO TARGET RECOGNITION WITH CR.....	43
D.	PWE AND WI WAVEFORM COMPENSATION	44
1.	Decreasing Range between the CR and Target.....	44
2.	Increasing Range between the CR and Target.....	47
E.	MOTION COMPENSATED WAVEFORMS	49
1.	Introduction.....	49

2.	Decreasing Range between the CR and Target – Wideband Waveform	49
3.	Decreasing Range between the CR and Target – Comparison between Compensated and Non-compensated Waveforms	50
4.	Increasing Range between the CR and Target – Comparison between Compensated and Non-compensated Waveforms	54
5.	P_{cd} for Decreasing Range - Comparison between Original and Compensated Waveforms	57
6.	P_{cd} for Increasing Range – Comparison between Original and Compensated Waveform	59
F.	CHAPTER SUMMARY.....	62
V.	CONCLUSIONS AND RECOMMENDATIONS.....	65
	LIST OF REFERENCES	67
	INITIAL DISTRIBUTION LIST	69

LIST OF FIGURES

Figure 1.	ANTR values for probability weighted energy (PWE) and wideband (WI) waveforms for a probability threshold of 0.9.....	17
Figure 2.	ANTR, P_{cd} , ApNTCD and MNTCD values obtained for the PWE waveform for a probability threshold equal to 0.90.....	20
Figure 3.	ANTR, P_{cd} , ApNTCD and MNTCD values obtained for the wideband waveform for a probability threshold equal to 0.9.....	20
Figure 4.	ANTR, P_{cd} , ApNTCD and MNTCD values obtained for the PWE waveform for a probability threshold equal to 0.95.....	21
Figure 5.	ANTR, P_{cd} , ApNTCD and MNTCD values obtained for the wideband waveform for a probability threshold equal to 0.95.....	21
Figure 6.	ANTR values obtained for the wideband and PWE waveforms for a probability threshold equal to 0.90.	22
Figure 7.	MNTR values obtained for the wideband and PWE waveforms for a probability threshold equal to 0.9	23
Figure 8.	P_{cd} obtained for wideband and PWE waveforms for 1, 2, 4, 10, 20 and 40 transmissions.....	24
Figure 9.	P_{cd} values obtained for PWE and wideband waveforms for different energy levels.	25
Figure 10.	P_{cd} and ACTP values obtained for the wideband waveform at different energy levels.	27
Figure 11.	P_{cd} and ACTP values obtained for the PWE waveform at different energy levels.	28
Figure 12.	ACTP values for PWE and wideband waveforms and for different energy levels.	29
Figure 13.	P_{cd} and ACTP levels obtained for PWE and wideband waveforms and different energy levels.....	30
Figure 14.	P_{cd} and ACTP levels obtained for the wideband waveform and 1 transmission.	31
Figure 15.	P_{cd} and ACTP levels obtained for the wideband waveform and 4 transmissions.....	32
Figure 16.	P_{cd} and ACTP levels obtained for the wideband waveform and 10 transmissions.....	32
Figure 17.	P_{cd} and ACTP levels obtained for the wideband waveform and 20 transmissions.....	33
Figure 18.	P_{cd} and ACTP levels obtained for the wideband waveform and 40 transmissions.....	33
Figure 19.	P_{cd} and ACTP values obtained for the wideband waveform and different number of transmissions.	34

Figure 20.	P_{cd} and ACTP values obtained for wideband and PWE waveforms and 1 transmission.	35
Figure 21.	P_{cd} and ACTP values obtained for wideband and PWE waveforms and 2 transmissions.	36
Figure 22.	P_{cd} and ACTP values obtained for wideband and PWE waveforms and 4 transmissions.	36
Figure 23.	P_{cd} and ACTP values obtained for wideband and PWE waveforms and 10 transmissions.	37
Figure 24.	P_{cd} and ACTP values obtained for wideband and PWE waveforms and 20 transmissions.	37
Figure 25.	P_{cd} and ACTP values obtained for wideband and PWE waveforms and 40 transmissions.	38
Figure 26.	P_{cd} and ACTP values obtained for PWE waveform and different number of transmissions.	38
Figure 27.	P_{cd} values obtained for the PWE waveform and 10 transmissions.	40
Figure 28.	P_{cd} , ANTR, ApNTCD and MNTCD values obtained for a probability threshold of 0.90 without limiting the number of transmissions.	41
Figure 29.	P_{cd} values obtained for “original” wideband, compensated wideband, “original” and compensated PWE waveforms with 2 transmissions and approaching target.	45
Figure 30.	P_{cd} values obtained for “original” wideband, non-compensated wideband, “original” and non-compensated PWE waveforms with 4 transmissions and approaching target.	45
Figure 31.	P_{cd} values obtained for “original” wideband, non-compensated wideband, “original” and non-compensated PWE waveforms with 10 transmissions and approaching target.	46
Figure 32.	P_{cd} values obtained for “original” wideband, non-compensated wideband, “original” and non-compensated PWE waveforms with 20 transmissions and approaching target.	46
Figure 33.	P_{cd} values obtained for “original” wideband, non-compensated wideband, “original” and non-compensated PWE waveforms with 2 transmissions and target moving away from radar.	47
Figure 34.	P_{cd} values obtained for “original” wideband, non-compensated wideband, “original” and non-compensated PWE waveforms with 4 transmissions and target moving away from radar.	48
Figure 35.	P_{cd} values obtained for “original” wideband, non-compensated wideband, “original” and non-compensated PWE waveforms with 10 transmissions and target moving away from radar.	48
Figure 36.	P_{cd} values obtained for “original” wideband, non-compensated wideband, “original” and non-compensated PWE waveforms with 20 transmissions and target moving away from radar.	49

Figure 37.	P_{cd} values obtained for compensated wideband waveform with 10, 20 and 30 transmissions and approaching target.	50
Figure 38.	P_{cd} levels obtained for compensated and non-compensated waveforms for 2 transmissions and approaching target.	52
Figure 39.	P_{cd} levels obtained for compensated and non-compensated waveforms for 4 transmissions and approaching target.	52
Figure 40.	P_{cd} levels obtained for compensated and non-compensated waveforms for 10 transmissions and approaching target.	53
Figure 41.	P_{cd} levels obtained for compensated and non-compensated waveforms for 20 transmissions and approaching target.	53
Figure 42.	P_{cd} values obtained for compensated and non-compensated waveforms with 2 transmissions and target moving away from radar.	55
Figure 43.	P_{cd} values obtained for compensated and non-compensated waveforms with 4 transmissions and target moving away from radar.	55
Figure 44.	P_{cd} values obtained for compensated and non-compensated waveforms with 10 transmissions and target moving away from radar.	56
Figure 45.	P_{cd} values obtained for compensated and non-compensated waveforms with 20 transmissions and target moving away from radar.	56
Figure 46.	P_{cd} values obtained for “original” wideband, compensated wideband, “original” PWE and compensated PWE waveforms for 2 transmissions and approaching target.	57
Figure 47.	P_{cd} values obtained for “original” wideband, compensated wideband, “original” PWE and compensated waveforms PWE for 4 transmissions and approaching target.	58
Figure 48.	P_{cd} values obtained for “original” wideband, compensated wideband, “original” PWE and compensated PWE waveforms for 10 transmissions and approaching target.	58
Figure 49.	P_{cd} values obtained for “original” wideband, compensated wideband, “original” PWE and compensated PWE waveforms for 20 transmissions and approaching target.	59
Figure 50.	P_{cd} values obtained for “original” wideband, “ original” PWE, compensated wideband and compensated PWE waveforms with 2 transmissions and target moving away from radar.	60
Figure 51.	P_{cd} values obtained for “original” wideband, “original” PWE, compensated wideband and compensated PWE waveforms with 4 transmissions and target moving away from radar.	60
Figure 52.	P_{cd} values obtained for “original” wideband, “original” PWE, compensated wideband and compensated PWE waveforms with 10 transmissions and target moving away from radar.	61

Figure 53.	P_{cd} values obtained for “original” wideband, “original” PWE, compensated wideband and compensated PWE waveforms with 20 transmissions and target moving away from radar.	61
------------	--	----

LIST OF TABLES

Table 1.	Experiment data (NC: non correct decision, C: correct decision)	18
----------	---	----

THIS PAGE INTENTIONALLY LEFT BLANK

LIST OF ACRONYMS AND ABBREVIATIONS

ACTP	Average Correct Terminal Probability
ANTR	Average Number of Transmissions
ApNTR	Approximate Number of Transmissions
ApNTCD	Approximate Number of Transmissions of Correct Decision
CR	Cognitive Radar
KB	Knowledge –Based
MHT	Multiple Hypothesis Testing
MI	Mutual Interference
MNTR	Mean Number of Transmissions
MNTCD	Mean Number of Transmissions Provide Correct Decision
NTR	Number of Transmissions
P_{cd}	Probability of Correct Decision
PDF	Probability Density Function
PWE	Probability Weighted Energy
PWSV	Probability Weighted Spectral Variance
SNR	Signal-to-Noise-Ratio
WI	Wideband waveform

THIS PAGE INTENTIONALLY LEFT BLANK

EXECUTIVE SUMMARY

Research on conventional radar systems gained tremendous attention after WWII and advanced radar technology is still a high priority research activity especially in the military sector. More recently a new type of radar has been introduced. Cognitive radar (CR) is a closed-loop radar system with many similarities to human cognition. CR uses waveforms on a continuous basis in order to gain a better sense of the surrounding environment. Thus using the data collected by the received echoes, CR improves its performance in real time.

This thesis examines the performance of a static CR system used for target recognition under various constraints. Initially, the assumption is that both target and radar are static, i.e. there is no relative motion. To yield classification performances, we set up and perform Monte Carlo simulation in which a radar tries to classify a target from a set of alternatives. Throughout this work, our simulation set assumes four known target responses and in each Monte Carlo trial, the radar tries to identify the target present via multiple hypotheses testing (MHT). We assume an initial probability of $\frac{1}{4}$. Mainly two types of waveforms are used: wideband and Probability Weighted Energy (PWE). One of the performance metrics calculated after a Monte Carlo simulation is the probability of correct decision (P_{cd}). For the PWE waveform, CR forms the initial waveform by summing individual matched waveform of each target scaled by the initial probabilities. Once measurements are received, initial probabilities are updated via Bayes' theorem. The updating of this probability by CR using the probability density functions (*pdfs*) of the received vectors in a closed-loop operation is a critical procedure. The maximum a posteriori (MAP) is used for detection and classification.

This thesis is divided into two research thrusts. First, we discuss two different methods for using a static target recognition CR system. One technique is to use a specific probability threshold (for instance, 0.95 probability) but without limiting the number of transmissions. Thus, we let the CR system transmit until it achieves this predefined threshold. The second method sets a limit on the number of pulsed transmissions but without any specific probability threshold to satisfy. For the first

technique, the performance metrics are given by the Average Number of Transmissions (ANTR) and the Mean Number of Transmission given Correct Decision (MNTCD). For the second technique, the performance metrics are given by probability of correct decision P_{cd} and Average Correct Terminal Probability (ACTP). In a Monte Carlo simulation, ACTP is the average of all final probabilities that are produced only when correct decisions or classifications are made in the experiments. From the result of our Monte Carlo simulations, we observe that the ACTP is always slightly higher than the P_{cd} . Thus, in order to achieve the desired P_{cd} value for the specific available energy and number of transmissions, we have to achieve a slightly higher value of ACTP. From the comparison of the P_{cd} for the two methods of utilizing the CR system, we conclude that it is better in terms of P_{cd} to use a specific number of transmissions rather than to have a preset probability threshold.

The second research thrust in this thesis is we allow for target's extent to change due to the motion of target in the target recognition application. Again we use a target recognition scenario with four hypotheses in our Monte Carlo simulations. The movement of the target can be either approaching the CR or moving away from the CR. We assume CR is static. As the target moves, its temporal and amplitude responses change. In the simulations, both the wideband and PWE waveforms must be adapted to reflect the target's movement. We observe that when radar does not compensate the waveform, the CR's performance in terms of P_{cd} suffers degradation for both wideband and PWE waveforms. In this case, the radar does not take into account the target's movement and as such the waveform is not modified. These unmodified waveforms are called "non-compensated" waveforms. We label "original" waveforms in our performance plots for the initial case where there is no relative motion between radar and target. In other words, performance due to "original" waveforms is only used for reference and not for performance comparison to "non-compensated" waveforms. To mitigate the performance degradation due to motion, we modify the wideband and PWE waveforms into what we refer to as "compensated" waveforms. In the simulation, we account for the change in target response to reflect the target's movement.

For the first motion model (in which the target approaches the radar) there is improved radar performance, in terms of the P_{cd} when both the compensated wideband waveform and PWE waveform are used. Moreover, the P_{cd} shows greater improvement when the compensated PWE waveform is used compared to the compensated wideband waveform. It is easily observed that the difference in P_{cd} between the compensated PWE and non-compensated PWE waveform is much greater than the difference between the compensated and non-compensated wideband waveforms. This result proves how highly effective the PWE waveform is compared to the wideband waveform.

For the second motion model (in which the target moves away from the radar) we also observe that the PWE compensated waveform offers superior performance in comparison to the wideband waveform. However, the improvement in terms of P_{cd} is less significant compared to the case when target is approaching the radar. This is because as the target moves away from the radar its impulse response becomes smaller. Moreover, another general observation is that for low energy values (less than -20dB energy units) the P_{cd} of the target is almost constant (about 0.25). The P_{cd} of 0.25 is the initial probability of the four target hypotheses in our simulation and therefore this probability observation is expected. For high values of energy the improvement of radar's performance in terms of P_{cd} is remarkable especially when the compensated PWE waveform is used. Thus, using the compensated version of the wideband and PWE waveforms we achieve better P_{cd} performance using less energy in both cases of target motion.

For all the results presented in this research we used Matlab for simulation in obtaining performance results. For each performance metric presented, a Monte Carlo simulation of 10000 iterations was implemented with different values of energy for different numbers of transmissions.

THIS PAGE INTENTIONALLY LEFT BLANK

ACKNOWLEDGMENTS

First, I would like to express my gratitude to my beloved country Hellas (Greece), and the Hellenic Navy for the opportunity to enhance my professional expertise at the Naval Postgraduate School.

I dedicate this work to my parents, Charalampos and Maria, for all the sacrifices they made in raising me and for teaching me the real values in life.

I also want to dedicate this work to my sister, Joanna and my brother, Harris, for their endless support and unfailing love in good and bad times.

THIS PAGE INTENTIONALLY LEFT BLANK

I. INTRODUCTION

A. BACKGROUND

In recent years several attempts have been made to improve the performance of radar systems used in surveillance, tracking and imaging operations not only in military sector but in the civilian sector. One of the latest approaches for achieving this goal is the introduction of a closed-loop radar system called cognitive radar (CR). The characteristics of CR system are illustrated in the following chapter. Waveform design optimization has become a tool for CR implementation. Bell in [1] introduced the use of Signal-to-Noise-Ratio (SNR) criterion for detecting a known target in Gaussian noise. Pillai introduced an algorithm in the case of signal-dependent clutter to form a finite-duration illumination in [2]. In case of a known target in signal-dependent interference an optimum matched waveform was illustrated in [3] and extended in [4] by Romero and Goodman. Furthermore, Kay addressed in [5] a waveform design for the Gaussian clutter and Gaussian distributed point target. An interesting way to improve the waveform to be used for a specific CR platform for target recognition was introduced by Goodman in [6] where SNR and mutual interference (MI)–based waveforms were tested. In this CR implementation multiple hypotheses testing (MHT) was used to determine the target from a set of possible alternatives via probability–weighted spectral variance (PWSV). A simpler and more effective waveform design technique called probability weighted energy (PWE) was introduced by Romero [7]. PWE is the technique that is utilized in this thesis to modify the transmit waveform for a moving target such that the performance degradation due to motion is mitigated.

B. THESIS OBJECTIVE

This thesis has two research thrusts. First, it shows two different ways of using a CR system introduced by Goodman in [6] for target recognition. The first technique is to set a probability threshold that a CR system uses to terminate illumination as previously used in [6]. This is called sequential hypothesis testing. In the second method the number of pulsed transmissions is fixed. For this research we use 1, 2, 4, 10, and 40

transmissions. Several conclusions are made from the comparison of the two techniques for low and high used energy levels.

Secondly, this thesis introduces an extension waveform design for static cognitive radar and moving extended target based on the approach illustrated by Romero in [8] to improve performance in terms of probability of correct decision (P_{cd}). In target recognition, we assume a target is present from various alternatives but we do not know which target is actually present. In other words, there is a number of hypotheses in which the radar must choose from to decide which target is present. For the simulations performed in this research work, we use only four different target models for the target recognition procedure. In case of moving extended target, the design of the waveform must take into account the increase or decrease of the target's response in time and amplitude [8]. When the target approaches the CR its effective response increases and when the target moves away from the CR its effective response decreases. This thesis shows that if the target response changes but the waveform design is not modified the P_{cd} drastically decreases. On the other hand, when the waveform design is adjusted the radar's performance in terms of P_{cd} is improved.

C. THESIS OUTLINE

This research is organized as follows. The theoretical background of CR is covered in Chapter II. The formulation of PWE technique is also discussed in Chapter II. A comparison of two approaches to using CR system for target recognition is discussed in Chapter III. Performance metrics such as the probability of correct decision (P_{cd}), the average correct terminal probability (ACTP) for wideband and PWE waveforms are presented in Chapter III. The ratio of correct decisions to the number of experiments in a Monte Carlo experiment is P_{cd} . In contrast, ACTP is the average of all final probabilities that are produced only when correct decisions or classifications are considered in the experiments. The case of a static target recognition CR and moving extended target using wideband and PWE waveforms is discussed in Chapter IV. For a target whose extent changes with motion, a CR system must compensate the waveforms in order to mitigate the effect on performance. The results from using compensated waveforms for several

energy levels and for different number of transmissions are shown in Chapter IV. Finally, conclusions and some recommendations for future research in the area of CR are presented in Chapter V.

D. APPROACH

For all the figures illustrated in this research, Monte Carlo simulations are used to obtain the results. In our Monte Carlo experiments, we allow 10000 trials where target present is randomly chosen and noise realization is allowed to vary. In the case of moving extended target, waveforms are modified to take into account the change (increase/decrease) of target's temporal and amplitude response.

THIS PAGE INTENTIONALLY LEFT BLANK

II. COGNITIVE RADAR AND PROBABILITY WEIGHTED ENERGY (PWE) WAVEFORM

The basic theory related to CR and PWE waveforms is provided in this chapter.

A. COGNITIVE RADAR CHARACTERISTICS

CR technology is relatively new for military and civilian applications. The CR closed-loop radar system is an intelligent system that continually updates understanding of its environment in order to accomplish its mission. Many CR characteristics differ from those of conventional radar. We will illustrate two of the characteristics shortly in the following paragraphs. Haykin in [9] illustrated the characteristics of CR system and analyzed the experimental results from a case study of a small target in sea clutter in detail.

1. Cognitive Signal Processing Cycle

Perception and decision-making procedures in cognitive radar share many similarities to human nature as described by Haykin in [9]. A human person uses his/her five senses to observe the surrounding environment, then tries to understand it and finally decides which of these five senses must be used in order to obtain a better picture of this environment. The same procedure is used by a CR system which bases its investigation of the environment on the data collected from the received signals via transmitted waveforms. The main difference between CR and conventional radar is that CR uses feedback in order to update its knowledge of the environment and improve its performance.

2. Radar-Scene Analysis

The second basic CR characteristic is radar-scene analysis. Based on this analysis, the radar will decide whether targets of interest exist in the area of operation or not. If targets are detected CR may perform the identification of these targets. This analysis is based on radar returns and other information about the environment, such as temperature,

humidity, pressure, sea state and wind [9]. Radar returns are environment responses to the radar's transmission.

B. PROBABILIY WEIGHTED ENERGY (PWE) WAVEFORM

In this thesis we use the probability weighted energy (PWE) SNR waveform to detect the target in our target recognition application. The metrics used for performance evaluation are probability of correct decision (P_{cd}) and Average Correct Terminal Probability (ACTP).

The most important contribution of the PWE waveform is that it eliminates the waveform search algorithm, which ensures the use of less computational resources compared to the PWSV [7]. This factor is critical in real time radar operations because of the limitations of radar resource.

C. PWE TECHNIQUE MATHEMATICAL BACKGROUND

Radar is used in target recognition applications. The system's main performance metric is the probability of correct decision (P_{cd}) or sometimes called probability of correct classification. In target recognition, we assume a target is present from various alternatives but we do not know which target is actually present. In other words, there are a number of hypotheses in which the radar must choose from to decide which target is present.

In order to produce P_{cd} we utilize Monte Carlo simulations in our target recognition problem and we assume four target possibilities which correspond to four hypotheses. In order to obtain numerical results for P_{cd} we use 10000 iterations in our Monte Carlo experiments. Moreover, we use four different known target responses. We assume that each target has an initial probability of 0.25. We form the initial waveform from the individual matched waveform for each of the four hypotheses [7]. We scale the individual matched waveform of each target by their corresponding probability and then we sum these individual waveforms to create the transmit waveform [7]. We continue by updating this probability using the *pdfs* of the received vectors in a closed-loop operation.

To facilitate our simulations, we use discrete-time signal models. Let x be the complex-valued transmit waveform, $h_n, n=1,2,3,4$ be the target responses and w be the white Gaussian noise from the receiver. In general the received signal is given by

$$y = h * x + w \quad (2.1)$$

where $(*)$ designates the convolution operation.

For convenience, we can specifically describe $h = \sqrt{E_h} \bar{h}$ such that E_h is the target response energy and \bar{h} is a unit energy vector [8]. Although not necessary, we assume that $E_h = E_{h1} = E_{h2} = E_{h3} = E_{h4}$, i.e. all the four possible targets have the same target response energy. Moreover, we can let $x = \sqrt{E_x} \bar{x}$ such that E_x is the transmit waveform energy and \bar{x} is a unit energy vector. Thus, the received signal is

$$y = \sqrt{E_h} \bar{h} * \sqrt{E_x} \bar{x} + w. \quad (2.2)$$

For the alternative hypothesis H , the received signal is of the form:

$$\begin{aligned} H_1 : y &= \sqrt{E_h} \bar{h}_1 * \sqrt{E_x} \bar{x} + w \\ H_2 : y &= \sqrt{E_h} \bar{h}_2 * \sqrt{E_x} \bar{x} + w \\ H_3 : y &= \sqrt{E_h} \bar{h}_3 * \sqrt{E_x} \bar{x} + w \\ H_4 : y &= \sqrt{E_h} \bar{h}_4 * \sqrt{E_x} \bar{x} + w. \end{aligned} \quad (2.3)$$

Thus, the general form is $y_n = \sqrt{E_h} \bar{h}_n * \sqrt{E_x} \bar{x} + w$ for $n=1,2,3,4$. If we let \bar{H} be the target response convolution matrix [8] and $y = \sqrt{E_h} \sqrt{E_x} \bar{H} \bar{x} + w$ then $y_n = \sqrt{E_h} \sqrt{E_x} \bar{H}_n \bar{x} + w$. Notice that, the received energy due to the echo alone (i.e., no noise) is given by $s = h * x$. In general $s_n = h_n * x$ and $E_s = E_x E_h (\bar{H} \bar{x})^\dagger (\bar{H} \bar{x}) = E_x E_h \bar{x}^\dagger \bar{H}^\dagger \bar{H} \bar{x}$ where $(^\dagger)$ represents the conjugate transpose or Hermitian operation. If we set $\bar{R} = \bar{H}^\dagger \bar{H}$ to be the autocorrelation of the target convolution matrix then the received energy due to the target echo for any target hypothesis is given by $E_{s,n} = E_h E_x \bar{x}^\dagger \bar{R}_n \bar{x}$. From [8], let q_n

be the individual waveform matched to the n th target. Thus, the initial transmit waveform

$x = \sqrt{E_x} \sum_{n=1}^{n=4} q_n \sqrt{P_n^0}$ where P_n^0 is the initial probability of the n th target. In order to update

the initial probabilities under the 4 hypotheses we need *pdfs* of the measurement after the K th transmission. After every signal reception the probability update is given by

$$P_n^{K+1} = p_n(y_1, y_2, \dots, y_k) P_n^0 \quad (2.4)$$

where p_n designates the *pdf* due to the n th target, $p_n(y_1, y_2, \dots, y_k)$ the *pdf* due to the n th target after the K th transmission, P_n^0 designates the initial probability of the n th target and P_n^{K+1} is the probability update after the K th transmission [7].

1. One Transmission Using the PWE Waveform

We assume noise to be additive white Gaussian given by the distribution $w \sim CN(0, \sigma^2 I)$ and thus the *pdf* expression of the received signal with an arbitrary target is given by

$$p(y|H) = \frac{1}{\pi^N \sigma^{2N}} \exp\left(-\frac{1}{\sigma^2} (y-s)^\dagger (y-s)\right). \quad (2.5)$$

For example, for hypothesis one the *pdf* expression is given by

$$p(y|H_1) = \frac{1}{\pi^N \sigma^{2N}} \exp\left(-\frac{1}{\sigma^2} (y-s_1)^\dagger (y-s_1)\right). \quad (2.6)$$

The term $(y-s)^\dagger (y-s)$ in equation (2.5), can be simplified to

$$(y-s)^\dagger (y-s) = y^\dagger y - y^\dagger s - s^\dagger y + s^\dagger s. \quad (2.7)$$

Taking into account the factor $\frac{-1}{\sigma^2}$ in equation (2.5), we have

$$\left[\left(\frac{-1}{\sigma^2}\right)((y-s)^\dagger (y-s))\right] = \left[\frac{1}{\sigma^2} y^\dagger s + \frac{1}{\sigma^2} s^\dagger y + \frac{-1}{\sigma^2} s^\dagger s + \frac{-1}{\sigma^2} y^\dagger y\right] \quad (2.8)$$

and accounting for the exponential part of (2.5) concludes to

$$\begin{aligned}
\exp\left[\left(\frac{-1}{\sigma^2}\right)((y-s)^\dagger(y-s))\right] &= \exp\left[\frac{1}{\sigma^2}y^\dagger s + \frac{1}{\sigma^2}s^\dagger y + \frac{-1}{\sigma^2}s^\dagger s + \frac{-1}{\sigma^2}y^\dagger y\right] \Rightarrow \\
\exp\left[\left(\frac{-1}{\sigma^2}\right)((y-s)^\dagger(y-s))\right] &= \exp\left[\frac{2}{\sigma^2}\text{Re}\{s^\dagger y\} - \frac{1}{\sigma^2}s^\dagger s - \frac{1}{\sigma^2}y^\dagger y\right] \Rightarrow \\
\exp\left[\left(\frac{-1}{\sigma^2}\right)((y-s)^\dagger(y-s))\right] &= \exp\left[\frac{2}{\sigma^2}\text{Re}\{s^\dagger y\} - \frac{1}{\sigma^2}|s|^2 - \frac{1}{\sigma^2}|y|^2\right].
\end{aligned} \tag{2.9}$$

Thus, equation (2.5) modifies to

$$p(y|H) = \frac{1}{\pi^N \sigma^{2N}} \exp\left(\frac{1}{\sigma^2}(2\text{Re}\{s^\dagger y\} - |s|^2 - |y|^2)\right). \tag{2.10}$$

Finally we have for each of the four target hypotheses:

$$p(y|H_1) = \frac{1}{\pi^N \sigma^{2N}} \left[e^{\left[\frac{2}{\sigma^2}\text{Re}\{s_1^\dagger y\}\right]} e^{-\frac{1}{\sigma^2}|s_1|^2} e^{-\frac{1}{\sigma^2}|y|^2} \right] \tag{2.11}$$

$$p(y|H_2) = \frac{1}{\pi^N \sigma^{2N}} \left[e^{\left[\frac{2}{\sigma^2}\text{Re}\{s_2^\dagger y\}\right]} e^{-\frac{1}{\sigma^2}|s_2|^2} e^{-\frac{1}{\sigma^2}|y|^2} \right] \tag{2.12}$$

$$p(y|H_3) = \frac{1}{\pi^N \sigma^{2N}} \left[e^{\left[\frac{2}{\sigma^2}\text{Re}\{s_3^\dagger y\}\right]} e^{-\frac{1}{\sigma^2}|s_3|^2} e^{-\frac{1}{\sigma^2}|y|^2} \right] \tag{2.13}$$

$$p(y|H_4) = \frac{1}{\pi^N \sigma^{2N}} \left[e^{\left[\frac{2}{\sigma^2}\text{Re}\{s_4^\dagger y\}\right]} e^{-\frac{1}{\sigma^2}|s_4|^2} e^{-\frac{1}{\sigma^2}|y|^2} \right] \tag{2.14}$$

The sum of all hypotheses probabilities is equal to 1. Thus, the constants can be dropped from the *pdfs*. Later on the *pdfs* can be rescaled such that the sum of the probabilities

equal 1. In (2.5) to (2.14) we assume that $\frac{1}{\pi^N \sigma^{2N}} = A$ and $e^{-\frac{1}{\sigma^2}|y|^2} = b$ are constant and

(2.5) simplifies to

$$\begin{aligned}
p(y|H) &= \frac{1}{\pi^N \sigma^{2N}} [e^{\frac{2}{\sigma^2} \text{Re}\{s^\dagger y\}} e^{\frac{-1}{\sigma^2} |s|^2} e^{\frac{-1}{\sigma^2} |y|^2}] \Leftrightarrow \\
p(y|H) &= A [e^{\frac{2}{\sigma^2} \text{Re}\{s^\dagger y\}} e^{\frac{-1}{\sigma^2} |s|^2} b] \Leftrightarrow \\
p(y|H) &= Ab [e^{\frac{2}{\sigma^2} \text{Re}\{s^\dagger y\}} e^{\frac{-1}{\sigma^2} |s|^2} b] \Leftrightarrow \\
p(y|H) &= Ab [e^{\frac{2}{\sigma^2} \text{Re}\{s^\dagger y\}} e^{\frac{-1}{\sigma^2} |s|^2}]. \tag{2.15}
\end{aligned}$$

From equation (2.15), the factor Ab is constant and can be eliminated. Thus, we have the scaled *pdf* expression to be

$$\tilde{p}(y|H) = e^{\frac{2}{\sigma^2} \text{Re}\{s^\dagger y\}} e^{\frac{-1}{\sigma^2} |s|^2}. \tag{2.16}$$

Taking the natural log version of equation (2.16) yields

$$\begin{aligned}
\ln[\tilde{p}(y|H)] &= \ln[e^{\frac{2}{\sigma^2} \text{Re}\{s^\dagger y\}} e^{\frac{-1}{\sigma^2} |s|^2}] \\
\ln[\tilde{p}(y|H)] &= \frac{2}{\sigma^2} \text{Re}\{s^\dagger y\} - \frac{1}{\sigma^2} |s|^2. \tag{2.17}
\end{aligned}$$

Knowing that all probabilities sum up to 1, we can remove the $\frac{1}{\sigma^2}$ factor and thus the rescaled *pdf* expression is given by

$$\hat{p}(y|H) = 2 \text{Re}\{s^\dagger y\} - |s|^2. \tag{2.18}$$

Finally for each hypothesis, we have

$$\hat{p}(y|H_1) = [2 \text{Re}\{s_1^\dagger y\}] - [|s_1|^2] \tag{2.19}$$

$$\hat{p}(y|H_2) = [2 \text{Re}\{s_2^\dagger y\}] - [|s_2|^2] \tag{2.20}$$

$$\hat{p}(y|H_3) = [2 \text{Re}\{s_3^\dagger y\}] - [|s_3|^2] \tag{2.21}$$

$$\hat{p}(y|H_4) = [2 \text{Re}\{s_4^\dagger y\}] - [|s_4|^2]. \tag{2.22}$$

2. K Number of Transmissions Using the PWE Waveform

Now we consider the *pdf* expression of the received signal for K transmissions. From the general equation for *pdf* with one transmission we have

$$p(y|H) = \frac{1}{\pi^N \sigma^{2N}} \exp\left(-\frac{1}{\sigma^2} (y-s)^\dagger (y-s)\right). \quad (2.23)$$

We assume that successive received measurements are independent so for K transmissions we multiply the *pdfs*. Thus, the *pdf* in (2.4) becomes

$$p_n(y_1, y_2, \dots, y_k) = p(y|H)_K = \prod_{i=1}^K \left[\frac{1}{\pi^N \sigma^{2N}} \exp\left(-\frac{1}{\sigma^2} (y_i - s_i)^\dagger (y_i - s_i)\right) \right]. \quad (2.24)$$

From (2.27) we let

$$\Psi = \frac{1}{\pi^{NK} \sigma^{2NK}} \quad (2.25)$$

From (2.10), we recall

$$p(y|H)_K = \prod_{i=1}^K \frac{1}{\pi^N \sigma^{2N}} \left[e^{\left[\frac{2}{\sigma^2} \text{Re}\{s_i^\dagger y_i\} \right]} e^{\frac{-1}{\sigma^2} |s_i|^2} e^{\frac{-1}{\sigma^2} |y_i|^2} \right]. \quad (2.26)$$

Replacing (2.25) into (2.10), (2.26) simplifies to

$$p(y|H)_K = \Psi e^{-\sum_{i=1}^K \frac{1}{\sigma^2} |y_i|^2} e^{2 \sum_{i=1}^K \frac{1}{\sigma^2} \text{Re}(s_i^\dagger y_i)} e^{-\sum_{i=1}^K \frac{1}{\sigma^2} |s_i|^2}. \quad (2.27)$$

The first two factors of equation (2.27) are again constant, thus we conclude that

$$p(y|H)_K = \Phi e^{2 \sum_{i=1}^K \frac{1}{\sigma^2} \text{Re}(s_i^\dagger y_i)} e^{-\sum_{i=1}^K \frac{1}{\sigma^2} |s_i|^2}. \quad (2.28)$$

where

$$\Phi = \Psi e^{-\sum_{i=1}^K \frac{1}{\sigma^2} |y_i|^2}, \quad (2.29)$$

so for each hypothesis, the final *pdf* expressions become

$$p(y|H_1)_K = \Phi e^{2\sum_{i=1}^K \frac{1}{\sigma^2} \text{Re}(s_{i,1}^\dagger y_i)} e^{-\sum_{i=1}^K \frac{1}{\sigma^2} |s_{i,1}|^2} \quad (2.30)$$

$$p(y|H_2)_K = \Phi e^{2\sum_{i=1}^K \frac{1}{\sigma^2} \text{Re}(s_{i,2}^\dagger y_i)} e^{-\sum_{i=1}^K \frac{1}{\sigma^2} |s_{i,2}|^2} \quad (2.31)$$

$$p(y|H_3)_K = \Phi e^{2\sum_{i=1}^K \frac{1}{\sigma^2} \text{Re}(s_{i,3}^\dagger y_i)} e^{-\sum_{i=1}^K \frac{1}{\sigma^2} |s_{i,3}|^2} \quad (2.32)$$

$$p(y|H_4)_K = \Phi e^{2\sum_{i=1}^K \frac{1}{\sigma^2} \text{Re}(s_{i,4}^\dagger y_i)} e^{-\sum_{i=1}^K \frac{1}{\sigma^2} |s_{i,4}|^2}. \quad (2.33)$$

Where $|s_{i,n}|^2$ corresponds to the received energy under the n th hypothesis. Recall, $n=1,2,3,4$. Taking the natural log of (2.28), we have

$$\ln(p(y|H)_K) = (\ln \Phi) \left(\frac{1}{\sigma^2} \right) \left\{ 2 \sum_{i=1}^K \text{Re}(s_i^\dagger y_i) - \sum_{i=1}^K |s_i|^2 \right\} \quad (2.34)$$

Dropping the constant $\ln \Phi \frac{1}{\sigma^2}$ in (2.34) yields the re-scaled *pdf* expression given by

$$\hat{p}(y|H)_K = 2 \sum_{i=1}^K \text{Re}(s_i^\dagger y_i) - \sum_{i=1}^K |s_i|^2. \quad (2.35)$$

Thus, for each hypothesis we have:

$$\hat{p}(y|H_1)_K = 2 \sum_{i=1}^K \text{Re}(s_{i,1}^\dagger y_i) - \sum_{i=1}^K |s_{i,1}|^2 \quad (2.36)$$

$$\hat{p}(y|H_2)_K = 2 \sum_{i=1}^K \text{Re}(s_{i,2}^\dagger y_i) - \sum_{i=1}^K |s_{i,2}|^2 \quad (2.37)$$

$$\hat{p}(y|H_3)_K = 2 \sum_{i=1}^K \text{Re}(s_{i,3}^\dagger y_i) - \sum_{i=1}^K |s_{i,3}|^2 \quad (2.38)$$

$$\hat{p}(y|H_4)_K = 2 \sum_{i=1}^K \text{Re}(s_{i,4}^\dagger y_i) - \sum_{i=1}^K |s_{i,4}|^2. \quad (2.39)$$

From [7], the $(K+1)$ th updated probability of the first hypothesis is

$$P_1^{K+1} = \beta P_1^0 \hat{p}(y|H_1)_K \quad (2.40)$$

where P_1^0 is the initial probability of the first hypothesis and P_1^{K+1} is the $(K+1)th$ updated probability of the first hypothesis and β ensures summation to unity. Thus, the updated probability for the n th hypothesis is given by

$$P_n^{K+1} = \beta P_n^0 \hat{p}(y|H_n)_K. \quad (2.41)$$

As for the PWE transmit waveform, the CR updates the transmission waveform to

$$x = \sqrt{E_x} \sum_{n=1}^{n=4} q_n \sqrt{P_n^K} \quad (2.42)$$

where P_n^K is the probability update prior to $(K+1)th$ transmission.

D. CHAPTER SUMMARY

In this chapter a short description of the CR characteristics was given and the similarity between human and CR dynamic closed-loop feedback system was illustrated. Furthermore, a discussion on the PWE waveform was provided along with the mathematical background. In the next chapter, a case study of two different ways to use a static target recognition CR will be illustrated. The first technique allows for a fixed energy to be transmitted. For a given energy, CR must approach a given threshold probability without limiting the number of transmissions. In contrast, the second technique CR utilizes a specific number of transmissions but without any particular probability threshold to satisfy. A comparison between the CR performance for these two techniques in terms of probability of correct decision (P_{cd}) and the average correct terminal probability (ACTP) for wideband and PWE waveforms will be presented. P_{cd} is the ratio of correct decisions to number of experiments in a Monte Carlo experiment and ACTP is the average of all final probabilities only when correct decisions or classifications are considered in the experiments.

THIS PAGE INTENTIONALLY LEFT BLANK

III. CLOSED-LOOP RADAR SYSTEM: A CASE STUDY OF TWO TECHNIQUES

A. INTRODUCTION

In this chapter we discuss two different ways to use a closed-loop radar system for target recognition first introduced in [6]. Just like in [6], we assume that both radar system and target do not move, i.e., are static. The first one is for a given energy, we let the CR approach a given probability threshold without limiting the number of transmissions the CR can use to satisfy this threshold. For simulation purposes of our target recognition problem, we again assume that the target present comes from four hypotheses of known target responses. We assume an initial probability of 0.25 for each hypothesis and we update this probability until the threshold we require is satisfied.

The second technique uses a fixed number of transmissions for a given fixed amount of energy per transmission. For the purposes of simulation we use 1, 2, 4, 10, 20 and 40 transmissions. In this case we do not have to satisfy a specific probability threshold. For each number of transmissions the radar decides which target is present by choosing the hypothesis with the largest final updated probability.

B. PROBABILITY THRESHOLD AND AVERAGE NUMBER OF TRANSMISSIONS (ANTR)

For the first method of using a target recognition CR system there is not a limit for the number of transmissions. In contrast, a specific probability threshold is set. Thus, we let the radar keep transmitting until it achieves this predefined threshold. For the simulation we set two values of probability threshold for two experiments. For the first simulation experiment the probability threshold is 0.90 and for the second simulation experiment the threshold is equal to 0.95. Two types of waveforms, wideband and PWE are used. After the Monte Carlo simulation, CR calculates the probability of correct decision. Initial target probabilities are assumed to be $\frac{1}{4}$. For the PWE waveform, CR forms the initial waveform from (2.47). The individual matched waveform is scaled by their corresponding update probability and the summation of these individual waveforms

is used to create the next transmit waveform. The updating of this probability by CR using the *pdfs* of the received vectors in a closed-loop operation is critical. The radar stops transmitting until one of the hypotheses reaches the threshold. The radar decides that the target corresponding to that hypothesis is the target present. The average number of transmissions (ANTR) is a performance metric shown in figures 1 to 5 for wideband and PWE waveforms. This metric is used to compare the CR's performance for the two different predefined probability thresholds of 0.90 and 0.95. ANTR is the average number of transmissions used to achieve the probability threshold. To present performance curves for the two waveforms, a Monte Carlo simulation of 10000 iterations was implemented for different energy values. The ANTR for wideband and PWE waveforms for energy values from -20dB to 0dB energy units and for probability threshold of 0.90 is shown in Figure 1. The green curve is for PWE and the blue curve is for the wideband waveform. We note that for both waveforms a high ANTR is needed to satisfy the requirement of 0.9 probability for low energy values. For instance, for a given energy of -20dB units we need 328 transmissions with the wideband waveform. On the other hand, for the PWE waveform we need only 203 transmissions, which indicate 40% savings compared to the ANTR of the wideband waveform. This reduction in transmissions proves the value of the PWE waveform. With both waveforms the ANTR necessary to satisfy the prerequisite requirement of 0.9 probability threshold is reduced when we increase the energy used. Thus, for high values of energy (more than -4dB energy units) the average number of transmissions for both cases is lower. Moreover, we notice the inferior performance of the wideband waveform compared to PWE. Notice the decrease in the ANTR necessary to satisfy the threshold condition between the two types of waveforms for every energy value. For instance, for -18dB energy units the difference in the number of transmissions is almost 66 transmissions (from 202 to almost 136) between the wideband and the PWE, but for a -12 dB energy units the difference is only 17 (51 - 34). The ANTR for a probability threshold of 0.90 for PWE and wideband waveform is shown in figures 2 and 3, respectively, and for the probability threshold of 0.95 the ANTR is shown in figures 4 and 5.

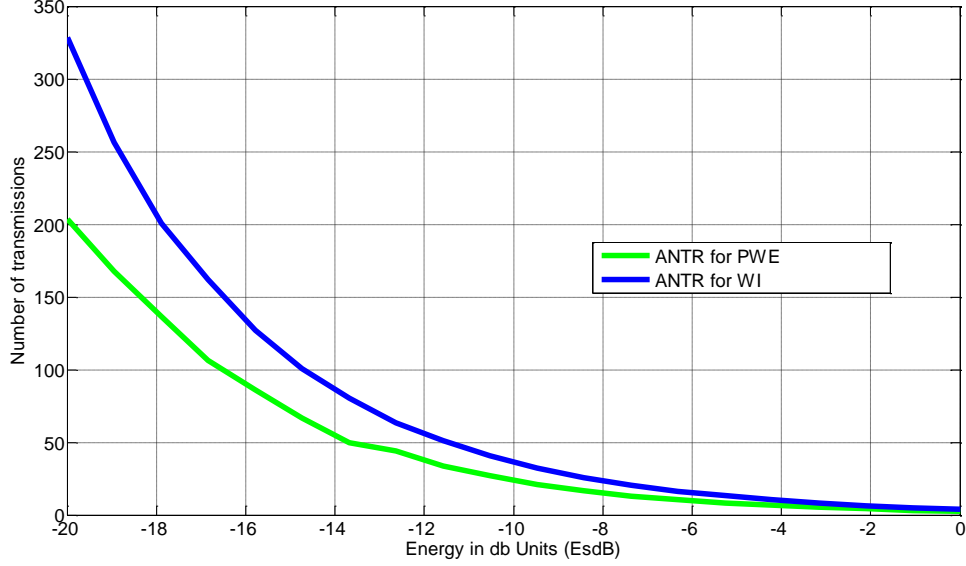


Figure 1. ANTR values for probability weighted energy (PWE) and wideband (WI) waveforms for a probability threshold of 0.9.

C. MEAN AND APPROXIMATE NUMBER OF TRANSMISSION GIVEN CORRECT DECISION

Here, we describe two performance metrics for radars performing target recognition: the approximate and the mean number of transmissions given correct decisions. Let us suppose that for a specific value of energy the probability of correct decisions is 0.75. Let us assume that the probability threshold is 0.9, and the resulting ANTR is 48 transmissions. Thus we might calculate the mean number of transmissions given correct decisions (MNTCD) by multiplying the probability of correct decisions times the ANTR. In this case 0.75×48 equals 36. However, this is a mistake because this number is merely an approximate number of transmissions (ApNTR) not the (MNTCD). We illustrate the difference by the following example.

Consider a radar system performing a total of six experiments as illustrated in Table 1. From the table, we can see that the probability of correct decision (P_{cd}) is 0.5. The average number of transmissions the radar system used for the six experiments is the summation of the transmissions for any experiment divided by the total number of experiments.

Thus, $Average = \frac{35+30+50+39+82+140}{6} = \frac{366}{6} = 61$ and the ApNTR given correct

decisions is the P_{cd} multiplied by ANTR. In other words, $P_{cd} * Average = 0.5 * 61 = 30.5$.

However, this is not the real mean value of transmissions given correct decisions. In order to find this number we have to add the number of transmissions of correct decisions and divide the sum by the number of experiments. Finally, we have

$Mean = \frac{30+39+140}{3} = \frac{209}{3} = 69.667$, which is different from 30.5 previously

calculated. Thus, to find the mean number of transmissions given correct decisions (MNTCD), we select experiments with correct decisions, find the number of transmissions corresponding to these experiments, sum these transmissions and divide it by the number of experiments with correct decisions.

Table 1. Experiment data (NC: non correct decision, C: correct decision)

Experiment	Exp1	Exp2	Exp3	Exp4	Exp5	Exp6
Number of Transmissions	25	30	50	39	82	140
Correct (C)/Not Correct Decision (NC)	NC	C	NC	C	NC	C

The ANTR, the P_{cd} and the average correct terminal probability (ACTP) for different values of energy for PWE and for wideband waveforms are shown in figures 2 and 3, respectively. ACTP is the average of all final probabilities that are produced only when correct decisions or classifications are made in the experiments.

The energy starts from very low values (-15dB energy units) to relatively high values (5dB energy units). We assume that the requirement is 0.9 probability threshold; the probability that one hypothesis reaches prior to making a decision. The first subplot in

Figure 2 (solid red curve) shows the ANTR needed to satisfy the 0.9 threshold, the second subplot (solid green curve) is the P_{cd} , the third subplot (solid pink curve) is the ApNTR given correct decisions and the last subplot (solid blue curve) is the MNTCD. From these subplots we observe that when the available energy is low the number of transmissions needed to satisfy our criterion (threshold 0.90) is high. Moreover, in this case CR achieves low values of P_{cd} . On the other hand, when the available energy is high the needed number of transmission is low and the values of P_{cd} are high. The same conclusion can be made for the wideband waveform. However, it is clear that the PWE waveform outperforms the wideband waveform. For instance, from low to high energy, the ANTR for PWE decreases from 72 to 2 while the ANTR for the wideband waveforms decreases from 108 to 2. Furthermore, the P_{cd} for PWE in Figure 2 starts at 0.38 and reaches almost 1 (100%). In contrast, for the wideband waveform in Figure 3 the P_{cd} starts at 0.38, but the highest value is 0.984. With both waveforms, if the number of transmissions is not limited, the ANTR given a specific probability threshold and the MNTCD are approximately the same as seen in first and fourth subplots of figures 2, 3, 4 and 5.

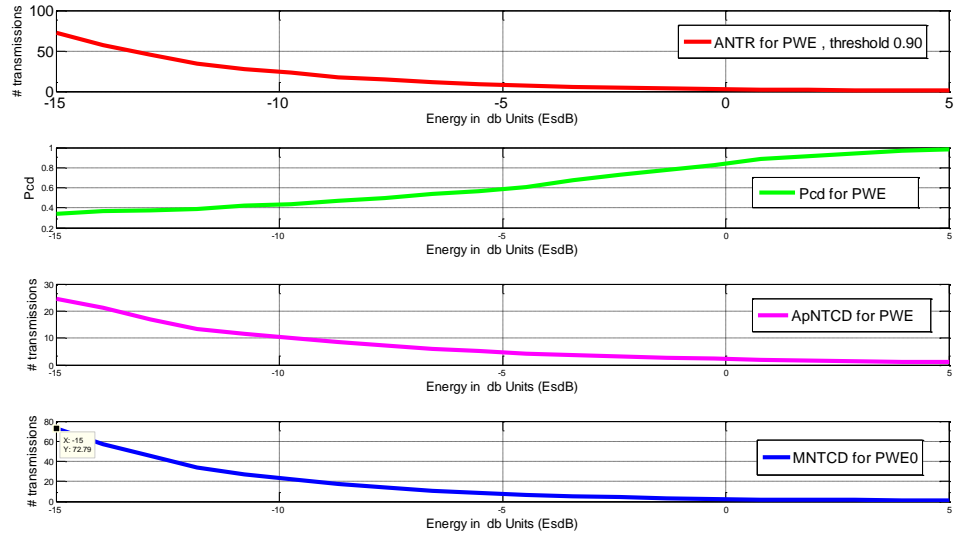


Figure 2. ANTR, P_{cd} , ApNTCD and MNTCD values obtained for the PWE waveform for a probability threshold equal to 0.90.

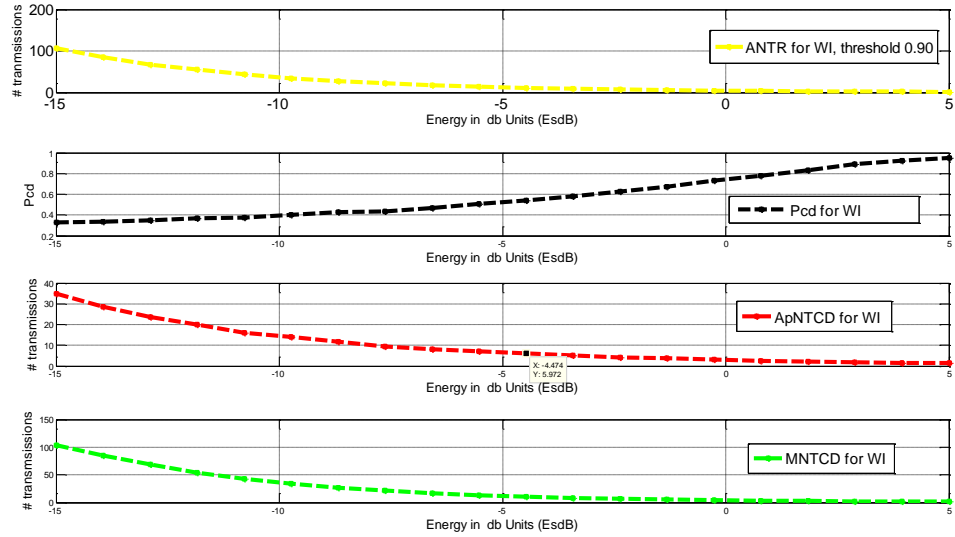


Figure 3. ANTR, P_{cd} , ApNTCD and MNTCD values obtained for the wideband waveform for a probability threshold equal to 0.9.

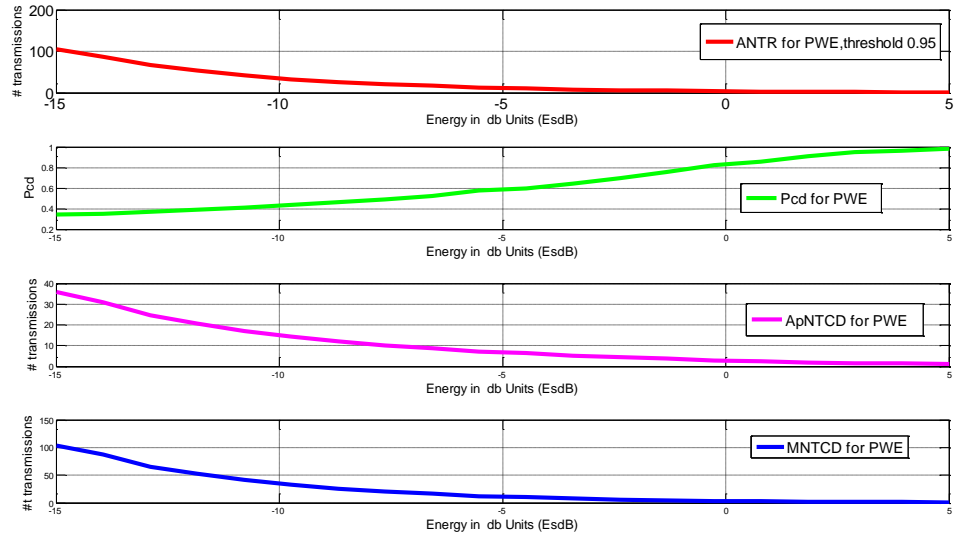


Figure 4. ANTR, P_{cd} , ApNTCD and MNTCD values obtained for the PWE waveform for a probability threshold equal to 0.95.

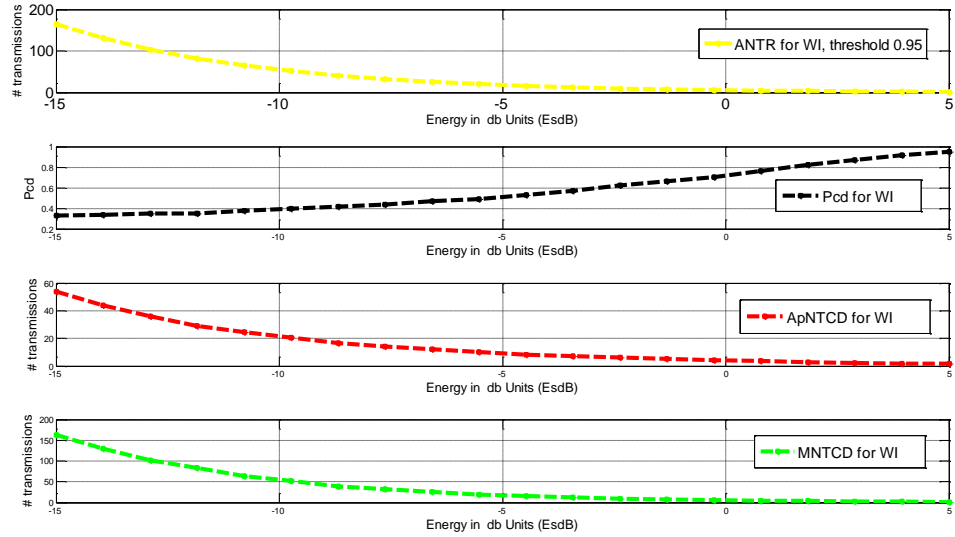


Figure 5. ANTR, P_{cd} , ApNTCD and MNTCD values obtained for the wideband waveform for a probability threshold equal to 0.95.

The ANTR with different values of energy for the two types of waveform is shown in Figure 6. Again we notice the inferior performance of the wideband waveform especially at low energy levels compared to the PWE waveform. This type of waveform needs a higher number of transmissions to satisfy the probability threshold of 0.9. For higher values of energy, the difference between the two ANTRs is gradually decreasing and for particularly high energy levels (above 0dB units) this difference is negligible.

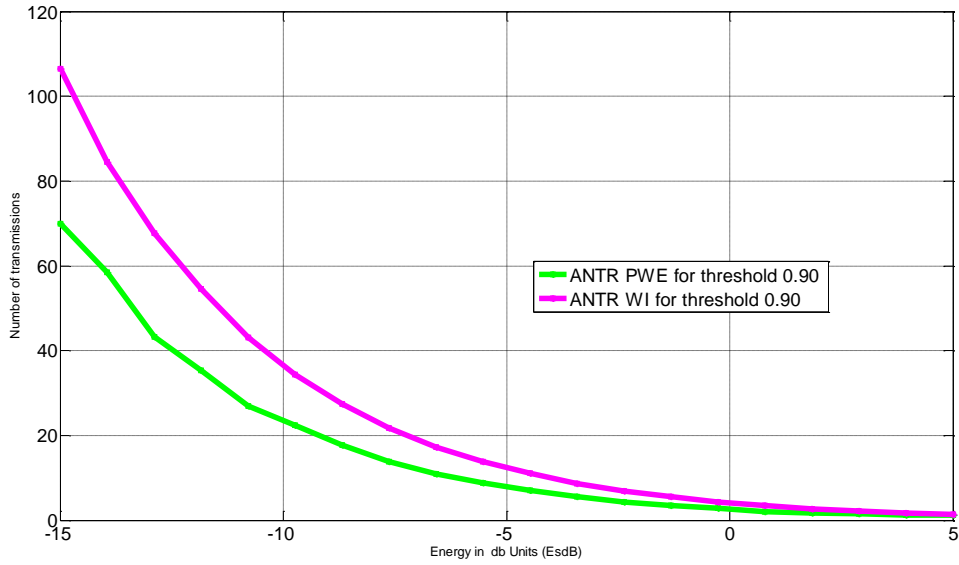


Figure 6. ANTR values obtained for the wideband and PWE waveforms for a probability threshold equal to 0.90.

The MNTR given correct decisions with different values of energy for the two types of waveforms is shown by Figure 7. The performance of the wideband waveform is worse than that of the PWE waveform.

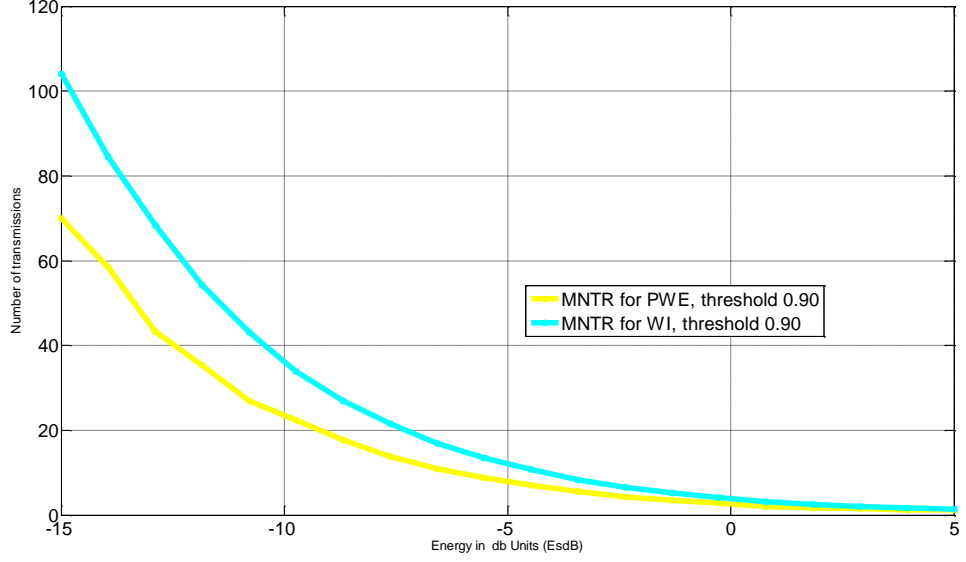


Figure 7. MNTR values obtained for the wideband and PWE waveforms for a probability threshold equal to 0.9

D. FIXED NUMBER OF TRANSMISSIONS

In any scenario that concerns detection or classification of a target, on sea, air or land, P_{cd} is a basic performance metric for a radar system (in this case a CR). However, P_{cd} depends on the number of transmissions and the energy of the transmitted signal. For the second method we do not use a specific probability threshold. In contrast, we use a specific number of transmissions; 1, 2, 4, 10, 20 and 40 transmissions. In our simulation, CR uses wideband and PWE waveforms and energy E equal to 1. The resulting P_{cd} for PWE and wideband pulsed waveforms is shown in Figure 8. As energy increases, the P_{cd} also increases, given a fixed number of transmissions. Notice that the PWE is clearly superior to the wideband waveform. For instance, in Figure 8 for the wideband waveform with an energy value of -10dB energy units and ten transmissions, the P_{cd} is equal to 0.68 (dashed dark blue curve). But for the PWE waveform with the same number of transmissions, the P_{cd} is equal to 0.82 (solid dark blue curve), which is a difference of almost 0.14. For a higher energy value of -5 dB energy units the P_{cd} is 0.9 for the wideband waveform and 0.98 for the PWE waveform, which is a difference of 0.18. In

contrast, for much lower values of energy, such as -25 dB energy units, the difference in P_{cd} for wideband and PWE is much smaller. Thus, we can conclude that for low energy levels the P_{cd} difference is small but as energy increases the P_{cd} increases. This is true for all six different values of transmissions: 1, 2, 4, 10, 20 and 40.

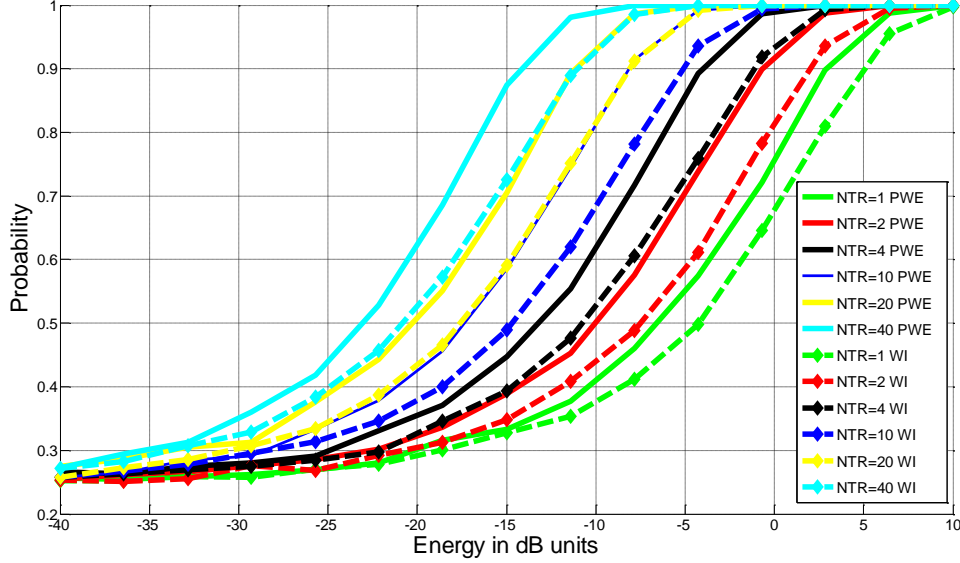


Figure 8. P_{cd} obtained for wideband and PWE waveforms for 1, 2, 4, 10, 20 and 40 transmissions.

In Figure 9, we plot the P_{cd} for energy values E equal to 0.001, 0.01, 0.1 and 1 for the number of transmissions from 0 to 40 for both waveforms. For all different values of energy the P_{cd} for the PWE waveform is higher than that for the wideband waveform. For the lowest energy level ($E=0.001$) the difference in the P_{cd} is almost negligible even for the highest transmission number. On the other hand, for the next energy level ($E=0.01$), as the number of transmissions is increased the difference between the P_{cd} for the PWE waveform and the P_{cd} for the wideband waveform is increased. For energy level equal to 0.1 (the pink and yellow curves for PWE and wideband waveforms respectively in Figure 9), the P_{cd} for the PWE is again higher than it is for the wideband waveform. We note that the difference between these probabilities is constantly increasing from 5

transmissions to 20 transmissions and is decreasing from 20 to 40 transmissions. For a high value of energy ($E=1$), the PWE still outperforms the wideband waveform. But after 10 transmissions both P_{cd} approach probability 1 and no performance gain is achieved by increasing the number of transmissions.

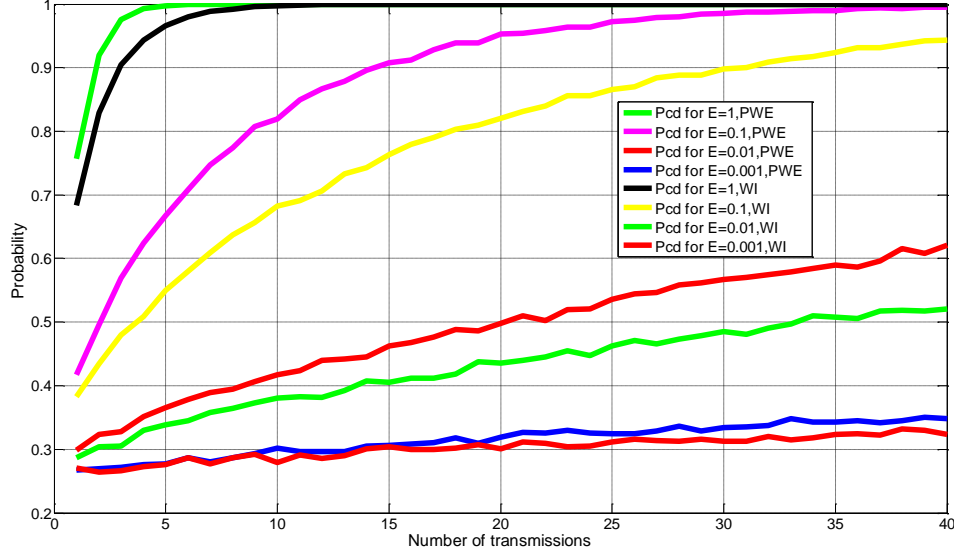


Figure 9. P_{cd} values obtained for PWE and wideband waveforms for different energy levels.

E. AVERAGE CORRECT TERMINAL PROBABILITY (ACTP)

1. Introduction

ACTP is a new performance metric introduced in this research. ACTP is slightly different from P_{cd} , which is the ratio of correct decisions to number of experiments in a Monte Carlo experiment. On the other hand, ACTP is the average of all final probabilities that are produced only when correct decisions or classifications are made in the experiments. For the illustrated plots in Figure 10 to Figure 28 a Monte Carlo simulation with 10000 trials with randomly chosen targets from our four hypotheses is performed. In our experiments, we let energy level be $E=0.001$, $E=0.01$, $E=0.1$ to $E=1$ and the number

of transmissions be from 0 to 40. From these figures we will show that P_{cd} is connected with the ACTP through a specific manner.

2. ACTP for WI Waveform

The resulting ACTP with energy values E equal to 1 (pink curve), 0.1 (red curve), 0.01 (blue curve) and 0.001 (cyan curve) for the number of transmission from 0 to 40 with the wideband waveform is shown in Figure 10. From this figure we can easily conclude that the higher the energy value, the higher the ACTP becomes given a fixed number of transmissions. We also see that as we increase the number of transmissions, ACTP increases for every energy level. Specifically, for the lowest value of energy ($E=0.001$) the ACTP ranges between 0.27 and slightly more than 0.33 (cyan curve). However, although we drastically increase the number of transmissions from 0 to 40, the ACTP does not significantly change. Therefore we conclude that for low energy levels, increase in transmission numbers does not increase the ACTP significantly. On the other hand, for the other three values of energy, increasing the number of transmissions results in the increase of ACTP. The most pronounced gain is obtained when the energy value E is equal to 0.1 where the ACTP increases from 0.38 to 0.95. In contrast, for the highest energy ($E=1$), we find that after 10 transmissions the ACTP does not change significantly with increasing number of transmissions since probability 1 is already reached. In other words, when the available energy E is equal to 1 and the required threshold for ACTP is greater than 0.95, we can stop after the tenth transmission. Thus we can save time and computational memory, which is something critical in real life operations.

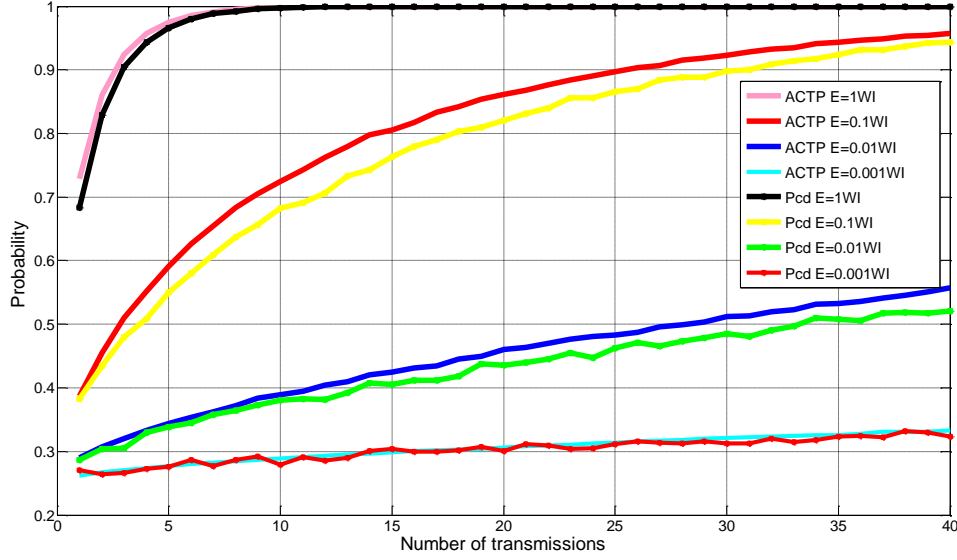


Figure 10. P_{cd} and ACTP values obtained for the wideband waveform at different energy levels.

3. ACTP for PWE Waveform

The resulting ACTP for PWE for values of energy E equal to 1 (blue curve), E equal to 0.1 (black curve), E equal to 0.01 (pink curve) and E equal to 0.001 (yellow curve) with the number of transmissions from 0 to 40 is shown in Figure 11. From this figure we can easily conclude that the higher the energy level is, the higher the ACTP is given a fixed number of transmissions. As the number of transmissions is increased, the ACTP increases for every energy level. Specifically, for the lowest value of energy ($E=0.001$), the ACTP ranges between 0.27 and 0.33 (solid yellow curve) which is a slightly better range compared to that of the wideband waveform. We conclude that for low energy levels the increase in transmission numbers does not affect the ACTP significantly. In contrast, for the other three values of energy, increasing the number of transmissions results in the increase of the ACTP. Again the most pronounced gain is for E equal to 0.1 (solid black curve) where the ACTP increases from 0.43 to 1. For the highest energy ($E=1$), we find that after five transmissions the ACTP almost reaches probability value of 1. In other words when the available energy E is equal to 1 and the required threshold for the ACTP is 0.95, we can stop at the fifth transmission.

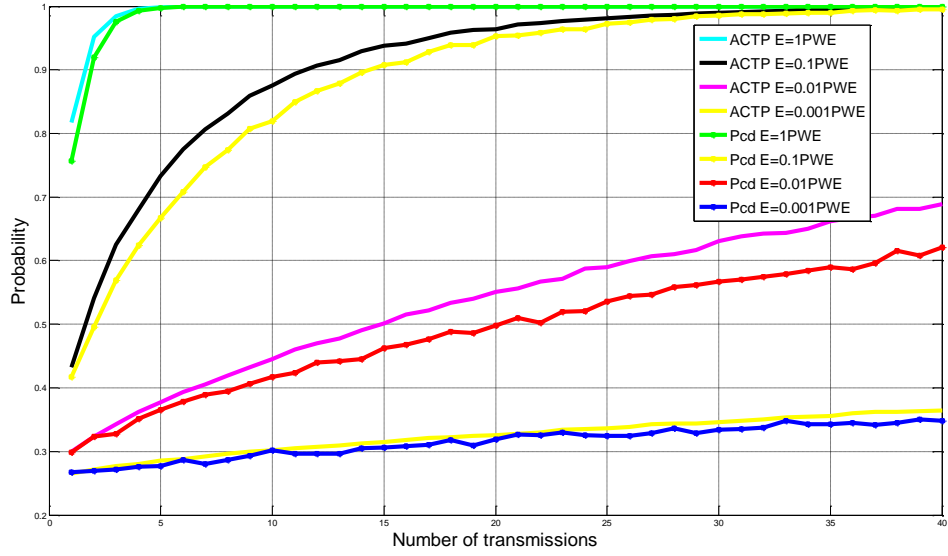


Figure 11. P_{cd} and ACTP values obtained for the PWE waveform at different energy levels.

A performance comparison between the PWE waveform and the wideband waveform using four different values of energy ($E=1$, $E=0.1$, $E=0.01$, $E=0.001$) for a number of transmissions ranging from 0 to 40 is shown in Figure 12. As we can see from this figure, the ACTP is higher for the PWE at all levels of energy with any number of transmissions, which simply indicates that the PWE technique highly improves the ACTP in comparison to the wideband waveform. However, a more detailed examination uncovers some interesting results. For the PWE waveform, the ACTP is higher for every number of transmissions when the energy level E is equal to 1 (see Figure 12, cyan curve) compared to other energy levels. From Figure 12 we conclude that for increased number of transmissions, not only the ACTP is increased but the difference in the ACTP between the PWE and wideband waveform is increased also.

For an energy value E equal to 0.1 we have a sharper improvement in the ACTP as we increase the transmission number (solid green and black curves in Figure 12). Furthermore, the PWE waveform shows a better performance compared with the wideband for all the transmission numbers. From Figure 12, if the available energy is lower than E equal to 1 we can achieve the previously defined ACTP threshold (ACTP=0.95) only with the PWE waveform and with an increased number of

transmissions ($NTR > 32$). In addition, the following curves in Figure 12 indicate that in the case of a high energy value ($E=1$) we can reach the highest ACTP threshold ($ACTP=1$) with a limited transmission number. In case of the PWE waveform ACTP equal to 1 can be achieved after the fifth transmission and ACTP equal to 1 can be achieved after the eighth transmission for the wideband waveform. The low demand on energy resource is highly desirable in real operations. Thus, for very low and for very high energy levels we do not have much ACTP gain. In contrast, for medium energy level the gain in terms of ACTP is remarkable.

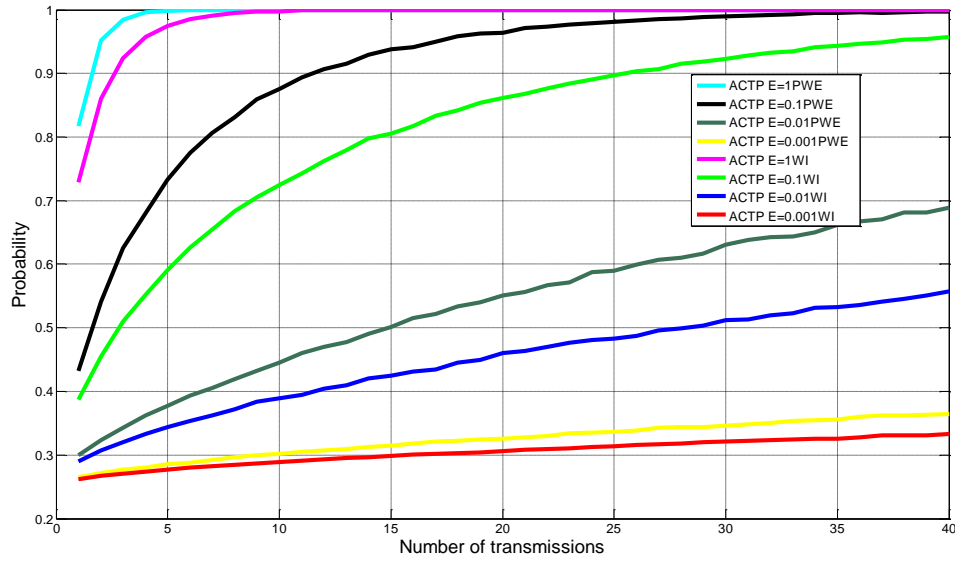


Figure 12. ACTP values for PWE and wideband waveforms and for different energy levels.

P_{cd} and ACTP levels obtained with different energy levels for number of transmissions from 0 to 40 for both waveforms are shown in Figure 13. Results show that for every energy level the ACTP is higher than the P_{cd} . However, the difference between the P_{cd} and the ACTP is negligible when the energy level is very low or very high. This is true for both the wideband and PWE waveform.

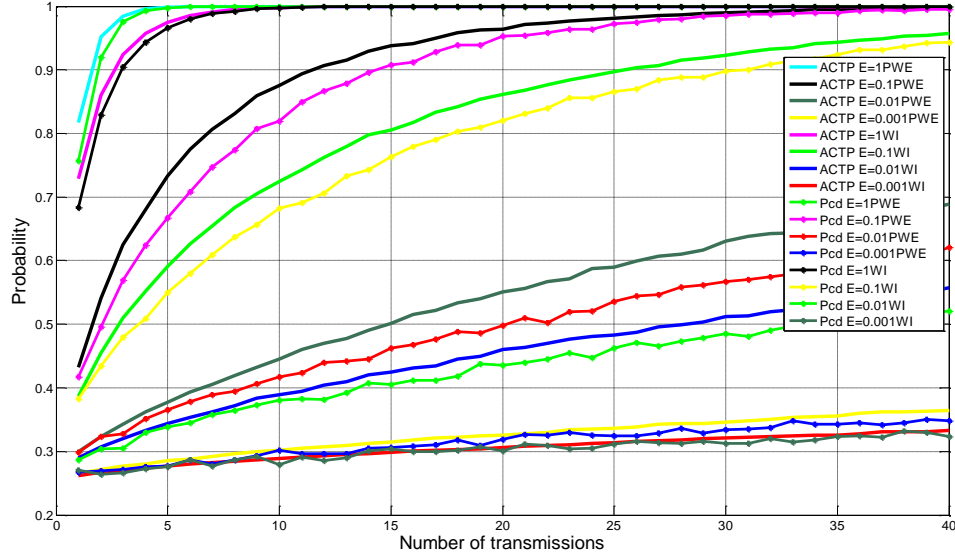


Figure 13. P_{cd} and ACTP levels obtained for PWE and wideband waveforms and different energy levels.

F. P_{cd} AND ACTP FOR WIDEBAND WAVEFORM

P_{cd} and ACTP values obtained for the wideband waveform are shown in Figure 14 to Figure 19. The energy varies from -40dB to 10dB units. We find that for low energy values (less than -10dB units) the P_{cd} and ACTP are almost the same. However, the increase in energy levels results in an increase in the P_{cd} and ACTP. Of course for a higher number of transmissions, a higher P_{cd} and higher ACTP, given the same energy value, are observed. For instance, for one transmission and for energy E equal to -10dB energy units, P_{cd} equal to 0.38, ACTP equal to 0.40 (Figure 14); but for 2 transmissions P_{cd} equal to 0.44 and ACTP equal to 0.46 (Figure 15). From figures 14 and 15, the ACTP is higher than the P_{cd} for the same value of signal energy. At very low energy levels the difference between the P_{cd} and the ACTP is negligible. However, as we increase the energy the difference increases even for a single transmission (Figure 14).

The ACTP is a metric that is different from the P_{cd} in the following way. Suppose we want to achieve a specific threshold of probability of correct decision of 0.80 with

twenty transmissions. As shown in Figure 17 we must use more than -10dB energy (dashed pink curve). However, from the yellow “diamond dashed” curve we can extrapolate that the ACTP is higher than 0.8; it is 0.85. Thus if we want to achieve a 0.8 P_{cd} we must achieve a 0.85 ACTP.

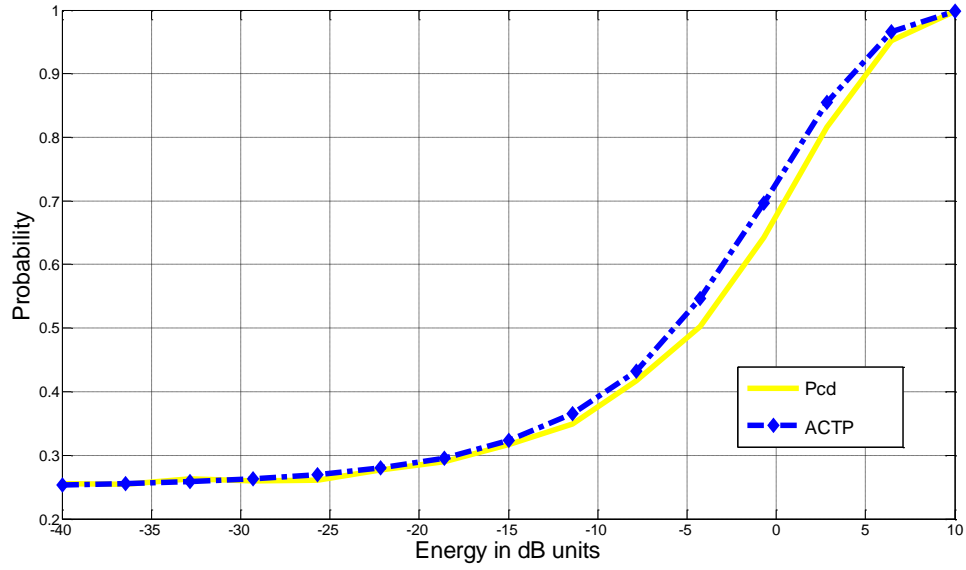


Figure 14. P_{cd} and ACTP levels obtained for the wideband waveform and 1 transmission.

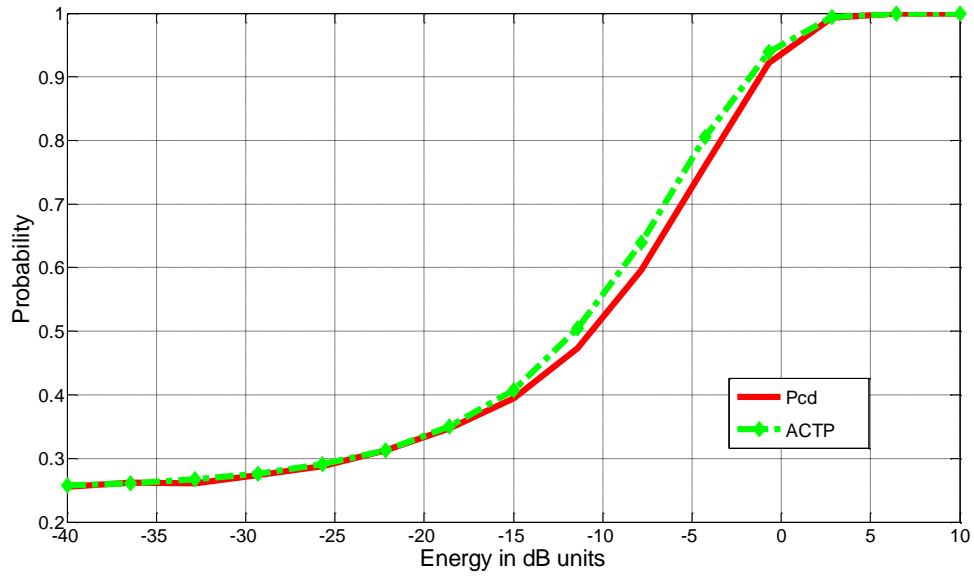


Figure 15. P_{cd} and ACTP levels obtained for the wideband waveform and 4 transmissions.

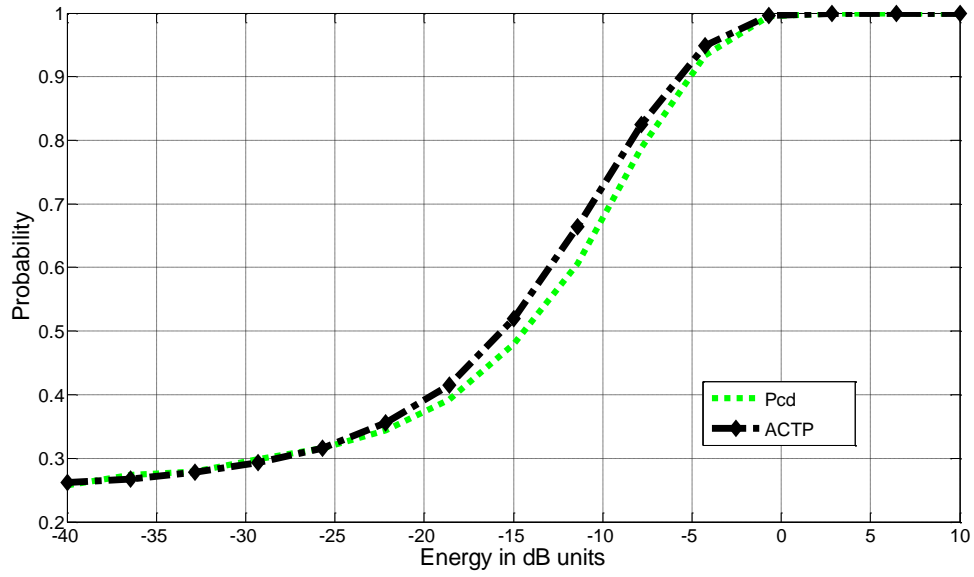


Figure 16. P_{cd} and ACTP levels obtained for the wideband waveform and 10 transmissions.

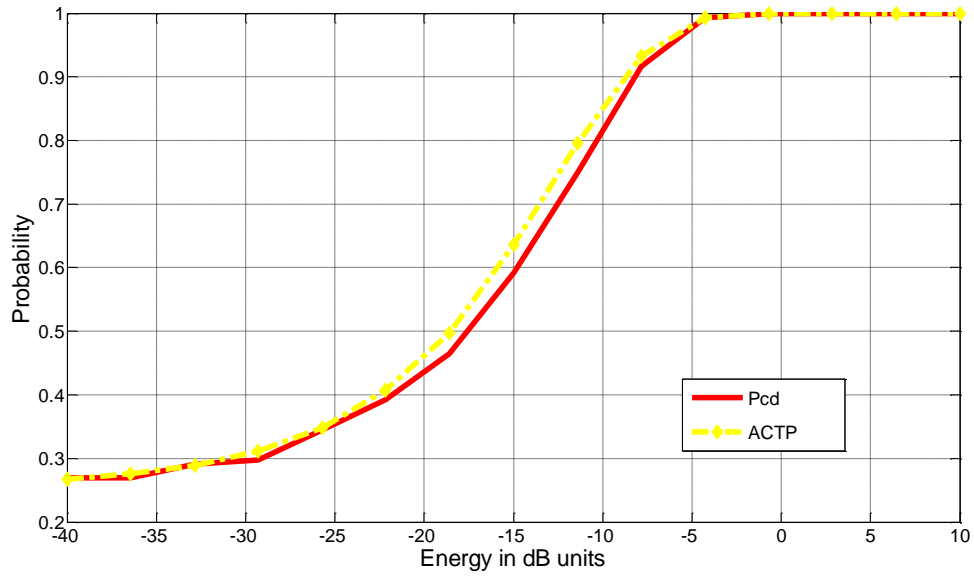


Figure 17. P_{cd} and ACTP levels obtained for the wideband waveform and 20 transmissions.

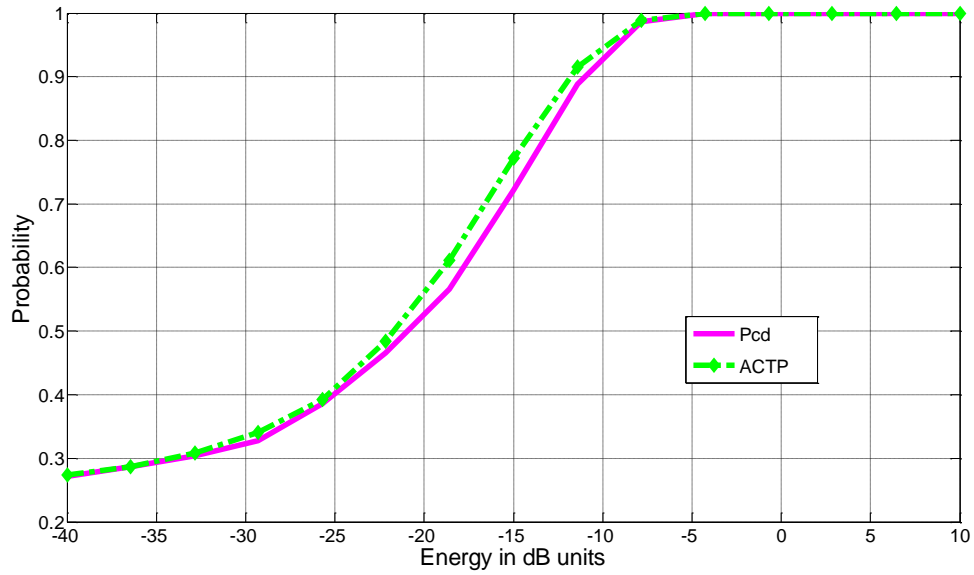


Figure 18. P_{cd} and ACTP levels obtained for the wideband waveform and 40 transmissions.

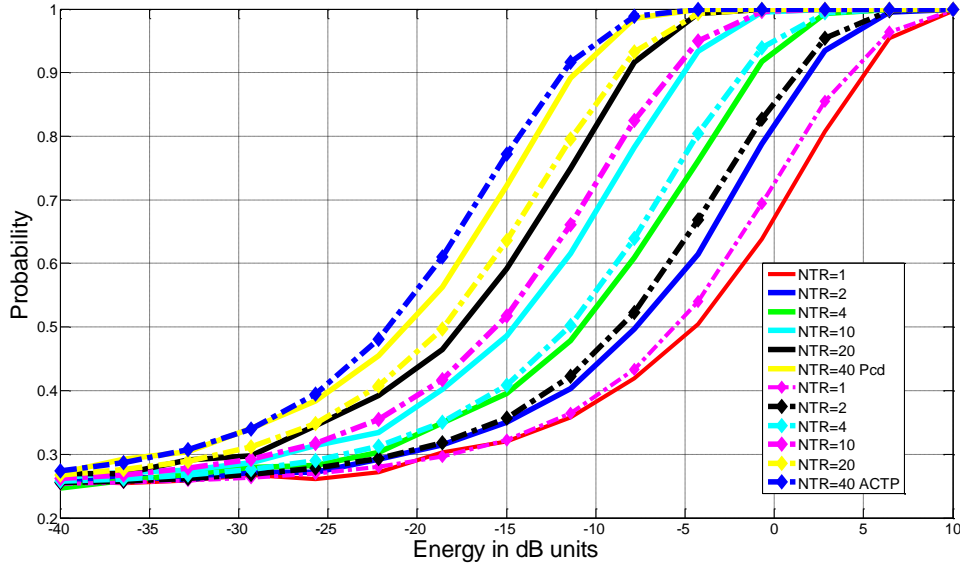


Figure 19. P_{cd} and ACTP values obtained for the wideband waveform and different number of transmissions.

G. P_{cd} AND ACTP FOR PWE WAVEFORM

In the following set of figures (Figure 20 to Figure 25) we plot the resulting P_{cd} and the ACTP obtained for the PWE and wideband waveform and 1, 2, 4, 10, 20 and 40 transmissions. Comparison between the P_{cd} and the ACTP for all six different values of transmission is shown in Figure 26. In these simulations, there is a fixed number of pulsed transmissions (1, 2, 4, 10, 20 and 40) but there is no specific probability threshold to satisfy. For all experiments, we use an energy constraint between -40dB to 10dB units and a Monte Carlo simulation of 10000 iterations. From figures 20 to 26 we can observe that the P_{cd} value obtained for the wideband waveform is lower than the P_{cd} level obtained for the PWE waveform, given a fixed number of transmissions for all energy values. Furthermore, the ACTP level for the wideband waveform is lower than the ACTP for the PWE technique. As energy increases for a given constant number of transmissions, P_{cd} and ACTP values increase for both PWE and wideband waveforms. Considering the

wideband waveform in Figure 22, we see that for four transmissions and signal energy of -15dB units, the P_{cd} level is equal to 0.4 and the ACTP value is equal to 0.42 (represented by the solid and dashed red curves, respectively). When the energy is increased to -5dB units, the P_{cd} level is equal to 0.72 and the ACTP value is equal to 0.8. Considering the same energy values with the PWE waveform, we see that the P_{cd} value improves from 0.43 to 0.88, and the ACTP improves from 0.48 to almost 0.9 (represented by the solid green and dashed black curves in Figure 22, respectively).

For completeness, we compile all P_{cd} and ACTP performances for both waveforms in Figure 26 for 1 to 40 number of transmissions. Both probabilities begin at 0.25. Moreover, results show for the same energy level P_{cd} and ACTP values also increase when the CR increases the number of transmissions. In the case of a high transmission number (that is, more than 15) P_{cd} and ACTP values are relatively high even when we use low energy levels.

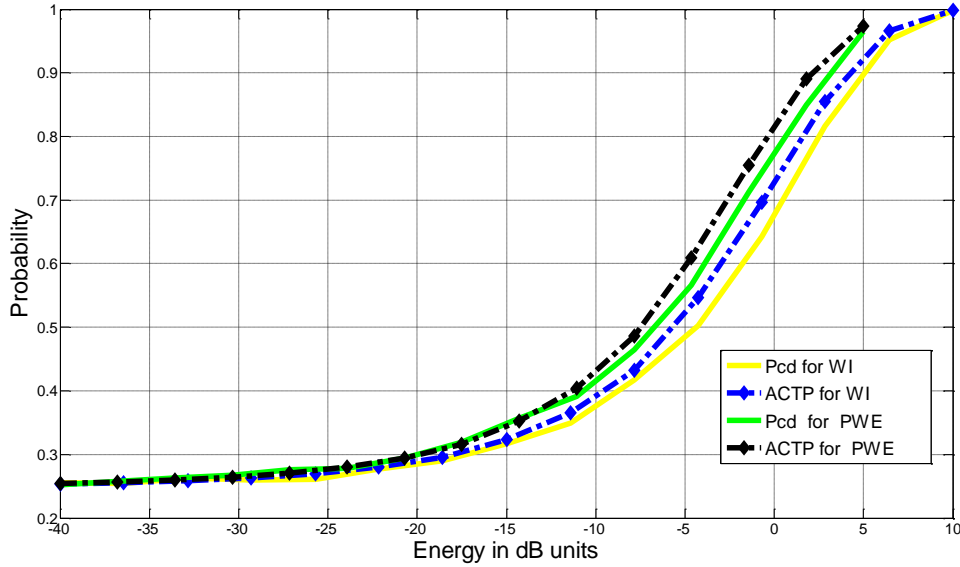


Figure 20. P_{cd} and ACTP values obtained for wideband and PWE waveforms and 1 transmission.

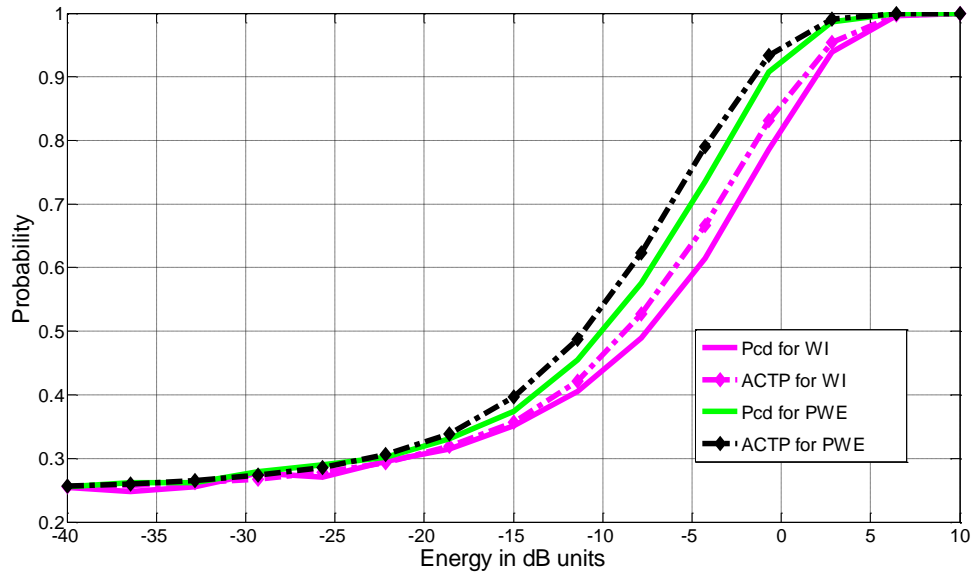


Figure 21. P_{cd} and ACTP values obtained for wideband and PWE waveforms and 2 transmissions.

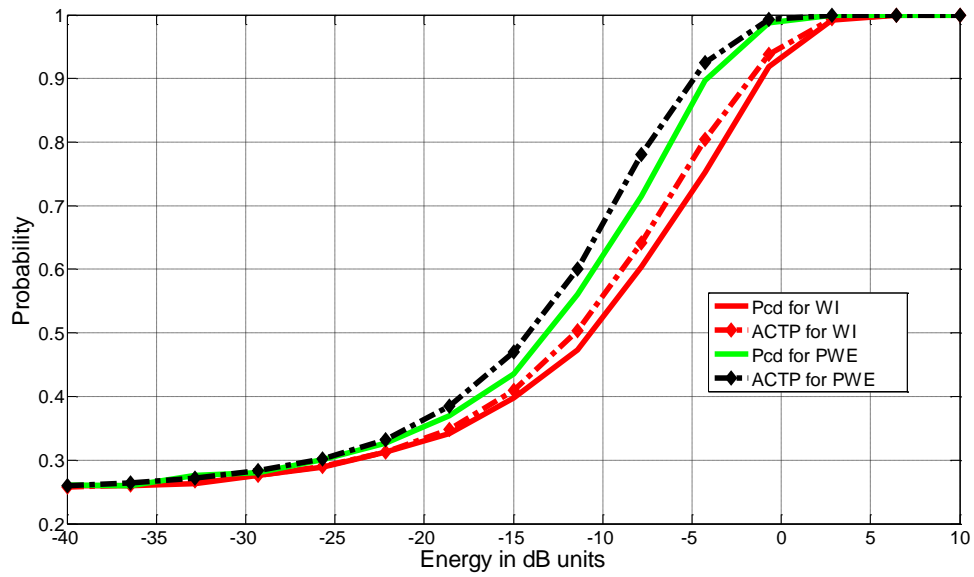


Figure 22. P_{cd} and ACTP values obtained for wideband and PWE waveforms and 4 transmissions.

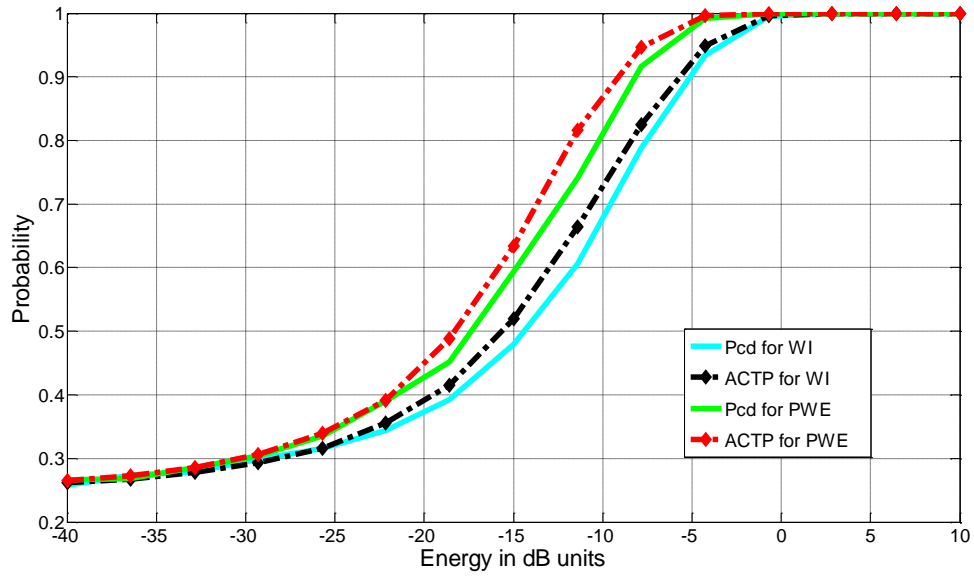


Figure 23. P_{cd} and ACTP values obtained for wideband and PWE waveforms and 10 transmissions.

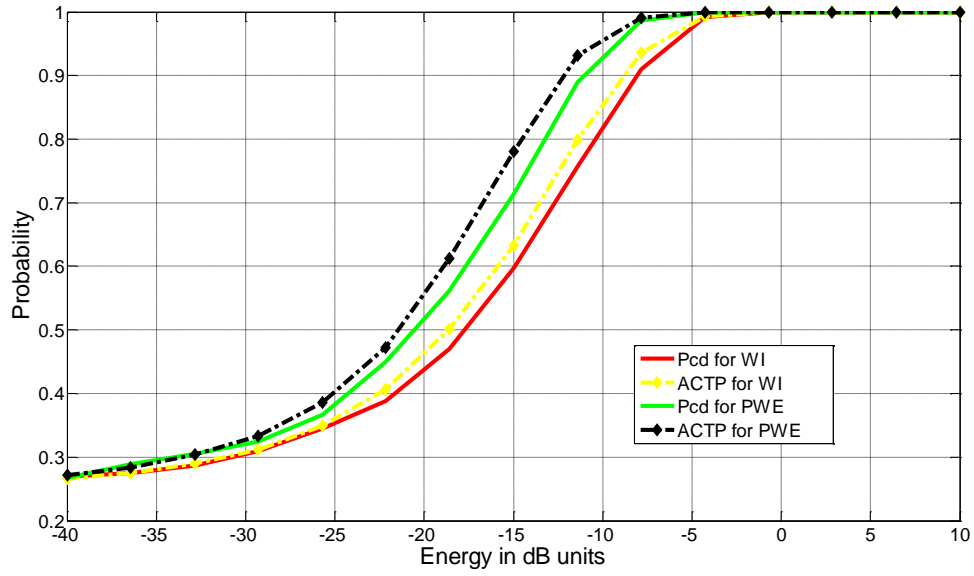


Figure 24. P_{cd} and ACTP values obtained for wideband and PWE waveforms and 20 transmissions.

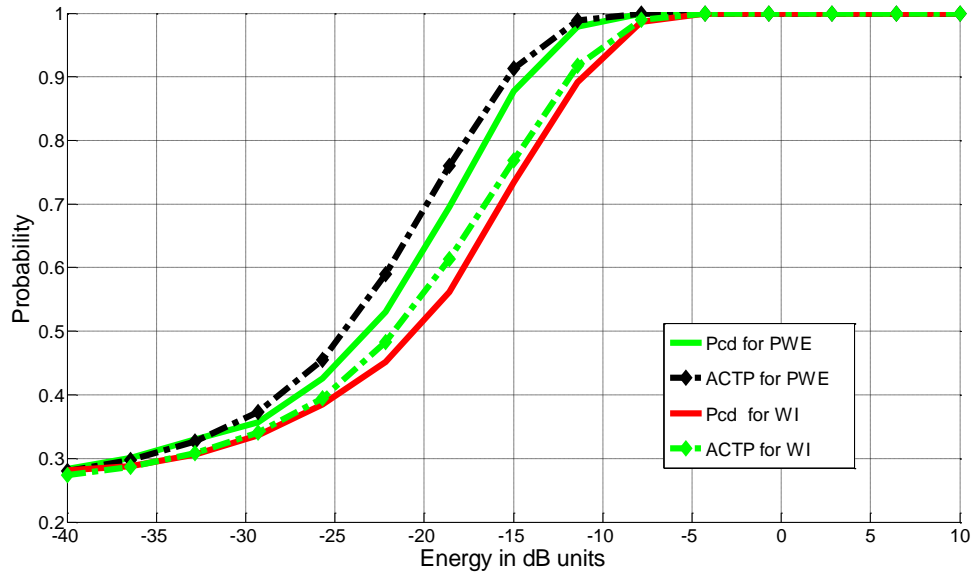


Figure 25. P_{cd} and ACTP values obtained for wideband and PWE waveforms and 40 transmissions.

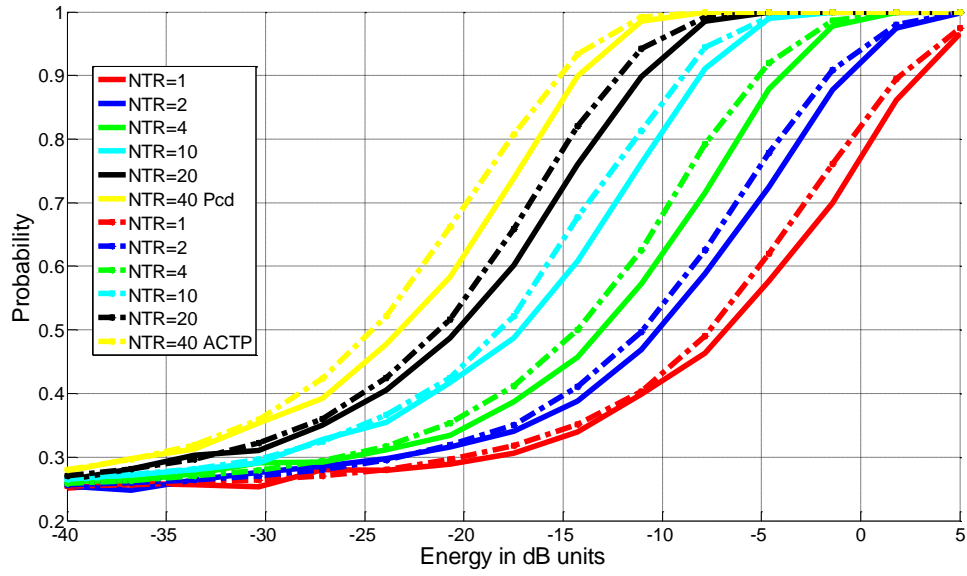


Figure 26. P_{cd} and ACTP values obtained for PWE waveform and different number of transmissions.

H. CHAPTER SUMMARY

This chapter discussed two approaches to use cognitive radar for target recognition. The first one sets a specific probability threshold without any limit on the number of transmissions the radar can use while the second one restricts the number of available transmissions to a predefined number.

Performance metrics for ACTP, ANTP, ApNTCD and MTNCD values were introduced. From the Monte Carlo experiments conducted, the ACTP is always higher than the P_{cd} for both the wideband and the PWE waveform. We also observed the performance superiority of the PWE waveform compared to that obtained with the wideband waveform using P_{cd} and ACTP as performance metrics. We concluded that to achieve a specific P_{cd} as a function of transmit energy given a fixed number of transmissions, we need a slightly higher value of the ACTP. In this way we can ensure to meet specific P_{cd} the system requires.

It is noteworthy to compare the two techniques for using CR. Consider figures 27 and 28. The P_{cd} in the case of a fixed number of transmissions (10 transmissions) is shown in Figure 27 where we can observe that even for low energy levels P_{cd} is relatively high. For instance for -15dB energy units P_{cd} is equal to 0.58. P_{cd} values obtained in the case of an unlimited number of transmissions but with a specific probability threshold to achieve (in this case 0.9) are presented in Figure 28. From this figure we observe that for low energy levels (although we have the ability to use unlimited number of transmissions) the system can not achieve a P_{cd} of 0.9 (the threshold we defined). The P_{cd} is low, which is less than 0.4 (solid green curve). For instance for -15dB units, P_{cd} is equal to 0.37 and the radar uses 73 transmissions (solid red curve). On the other hand, for a fixed number of transmissions (Figure 28), the P_{cd} for the same energy value (-15dB units) is equal to 0.58, which is a difference of almost 0.2 in probability. Moreover, the number of transmissions is extremely low, only 10 transmissions as compared to 73. Thus we conclude that it is better to use a specific number of transmissions with low energy signal levels. In both cases the increase in signal energy results in an increase in P_{cd} levels.

We should note that for higher energy levels we have different results. Specifically, with 0dB energy level when CR uses 10 transmissions, the P_{cd} is equal to 1 (the solid blue curve in Figure 28). In contrast, for the same energy level when the CR has to satisfy the 0.9 probability threshold without limiting the number of transmissions the value of P_{cd} is different. In this case from the solid green curve in Figure 28 we extract that P_{cd} is equal to 0.84. From the red solid curve in the same figure we observe that for P_{cd} equal to 0.84 CR used only 4 transmissions. Another observation from Figure 28 is that for energy level higher than 0dB units, the values of P_{cd} are between 0.8 and 1. And the number of transmissions to achieve these values of P_{cd} are much lower than 10. For high energy levels and probability threshold is set, CR achieves P_{cd} values close to 1 only by not limiting the number of transmissions. As stated before, for the same energy of 0dB units P_{cd} is equal to 1 using fixed number of transmissions (Figure 27), but with unlimited number of transmissions P_{cd} is equal to 0.84 (ANTR=4 transmissions). Thus, CR effectively saved 6 transmissions (10-4) for the same energy.

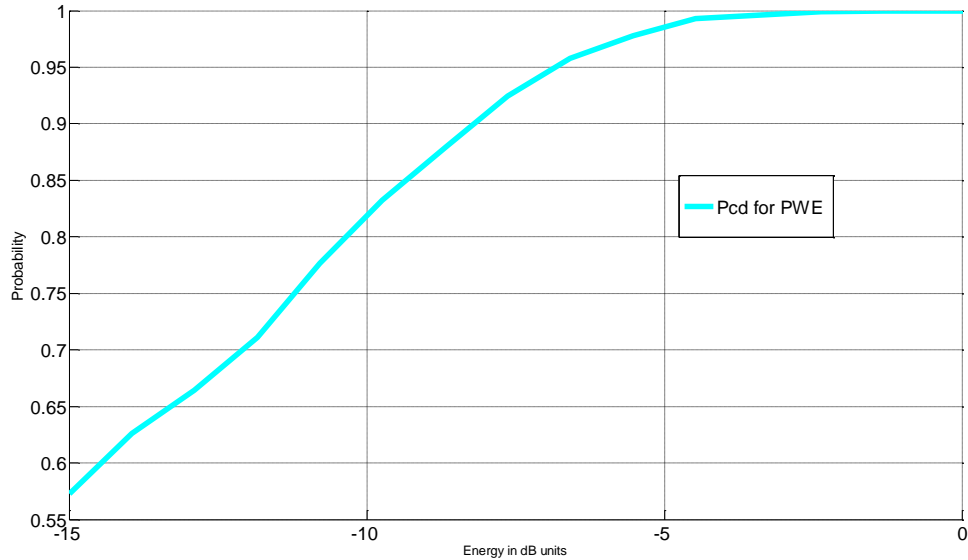


Figure 27. P_{cd} values obtained for the PWE waveform and 10 transmissions.

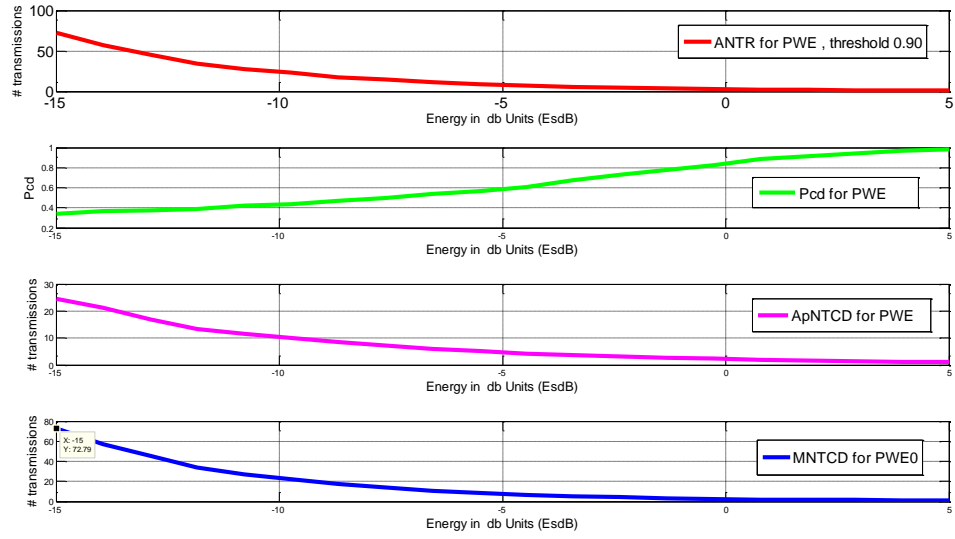


Figure 28. P_{cd} , ANTR, ApNTCD and MNTCD values obtained for a probability threshold of 0.90 without limiting the number of transmissions.

THIS PAGE INTENTIONALLY LEFT BLANK

IV. PROBABILITY OF CORRECT DECISION (P_{cd}) FOR MOVING EXTENDED TARGETS

A. INTRODUCTION

Recall that the scenarios described in the previous chapters consider the case when the radar and the target are static. Now we consider the case when the radar or target may be in motion. Waveform design compensation due to changes in target response due to motion between radar and extended target in terms of detection is initially discussed in [8]. In this thesis, we consider the two cases of a target moving either away from and moving directly toward the static radar in our target recognition problem.

B. CONCEPT APPROACH

In case of a moving target, its return changes compared with a stationary one. As discussed in [8] the range between static radar and moving target changes, i.e., the target's effective impulse response in time and amplitude changes. When the target approaches the static radar its impulse response increases in time and amplitude. In contrast, when the target moves away its impulse response decreases. Thus, when there is relative motion between radar and target the waveform design should be adjusted to compensate for these changes.

C. EXTENSION TO TARGET RECOGNITION WITH CR

In this thesis, we consider the case where the target is in motion and the radar is static. If the target moves away from the radar its amplitude and time extent become smaller but when the target approaches the radar its amplitude and time extent become greater. In our simulation, we have to account for these changes. For instance when target moves away from CR its impulse response h in equation (2.1) becomes smaller. In contrast, when the target approaches the static CR h becomes greater. Thus, equations (2.1) to (2.5) are modified. Since the probability of each hypothesis should be updated using the *pdfs* of the received vectors, equations (2.36) to (2.41) are modified and the waveforms are compensated.

D. PWE AND WI WAVEFORM COMPENSATION

To modify the PWE and wideband waveforms to adjust to the target's movement we have to account for our target's response in our simulation. Thus, if the waveform is not compensated, then CR's performance suffers [8]. However, because of target's motion the *pdfs* should be adjusted in every transmission. For each plot in figures 29 through 53, 10000 Monte Carlo trials are used. The curve labeled "original" refers to the case when the target and radar are static from the previous chapters. The performance curve is shown only for the purposes of comparison to the performance of the uncompensated waveforms labeled "non-compensated." The performance of the compensated waveforms is labeled "compensated". In the following paragraph we illustrate the losses in P_{cd} when CR uses the non-compensated waveforms.

1. Decreasing Range between the CR and Target

The performance of the non-compensated waveforms compared with the "original" performance, for 2, 4, 10 and 20 transmissions is shown in figures 29, 30, 31 and 32 respectively. In this series of simulation experiments, the target approaches the CR system. The performance labeled "original" actually refers to the case of both static target and radar. Here, we only use it as reference curve in order to illustrate the performance degradation due non-compensated waveforms. Recall that the non-compensated waveforms are used for the case of static radar and moving target.

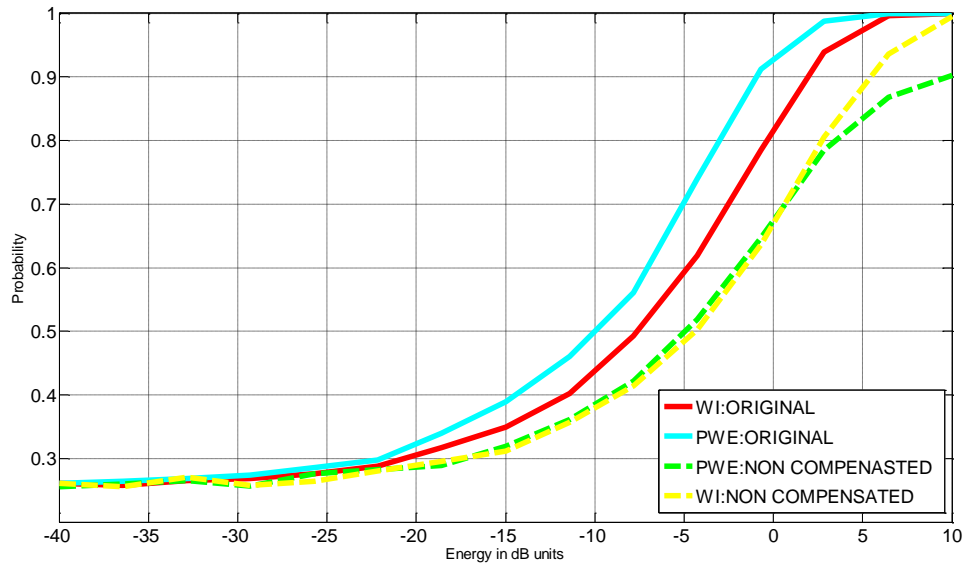


Figure 29. P_{cd} values obtained for “original” wideband, compensated wideband, “original” and compensated PWE waveforms with 2 transmissions and approaching target.

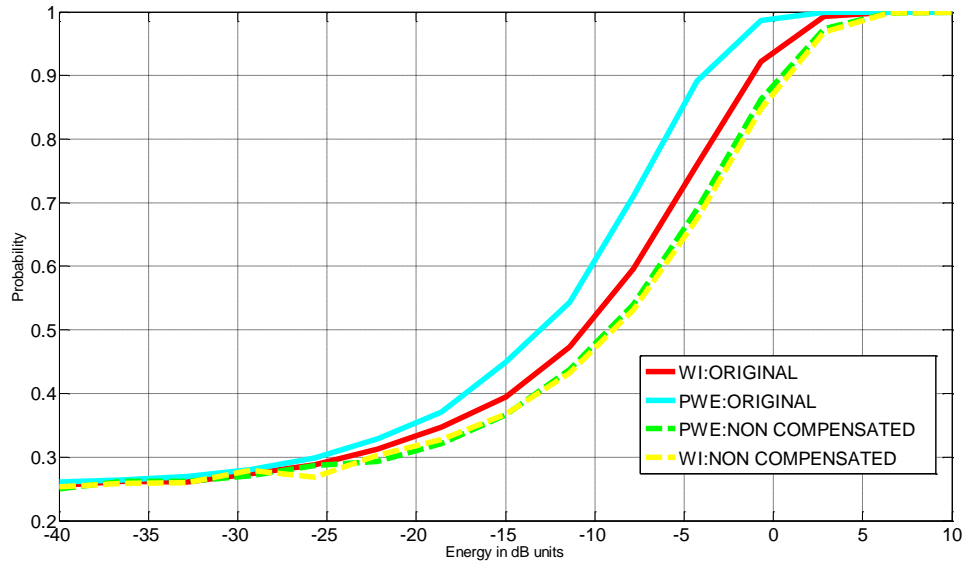


Figure 30. P_{cd} values obtained for “original” wideband, non-compensated wideband, “original” and non-compensated PWE waveforms with 4 transmissions and approaching target.

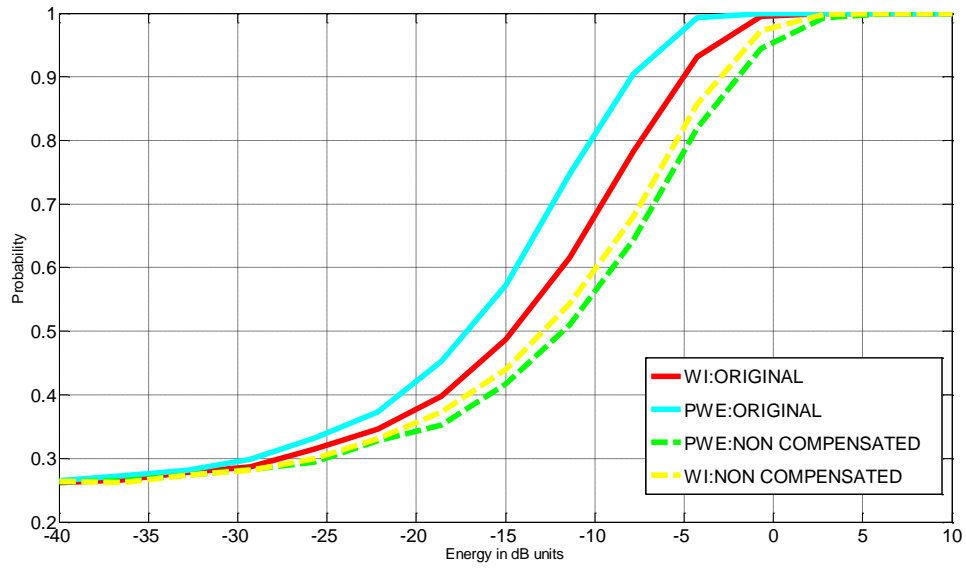


Figure 31. P_{cd} values obtained for “original” wideband, non-compensated wideband, “original” and non-compensated PWE waveforms with 10 transmissions and approaching target.

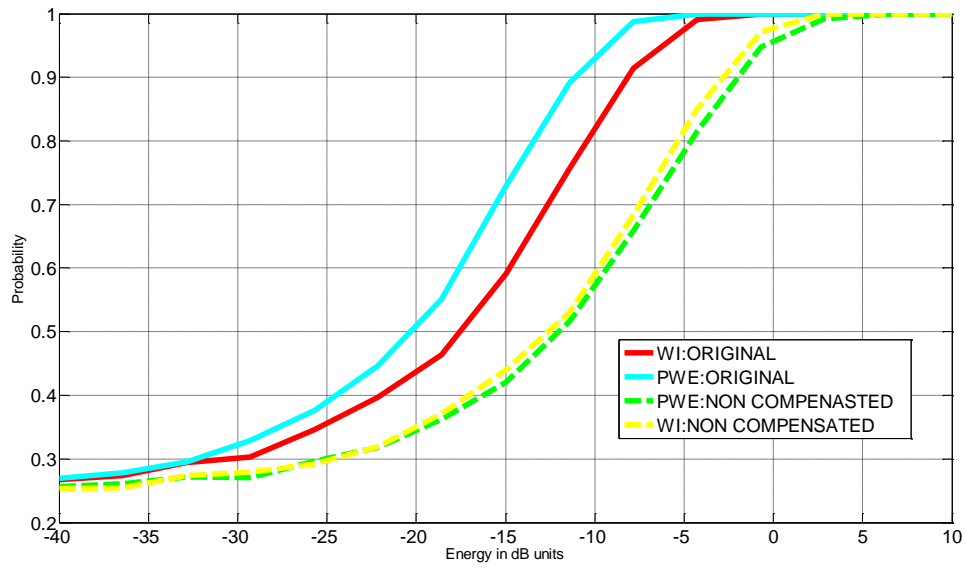


Figure 32. P_{cd} values obtained for “original” wideband, non-compensated wideband, “original” and non-compensated PWE waveforms with 20 transmissions and approaching target.

2. Increasing Range between the CR and Target

Here the CR system is static and the target is moving away. Because of target's motion its extent in time and amplitude is smaller. Again, we investigate the performance gain of compensated waveform and the performance loss of non-compensated waveforms. The loss is shown in figures 33, 34, 35 and 36 (for 2, 4, 10, and 20 transmissions, respectively).

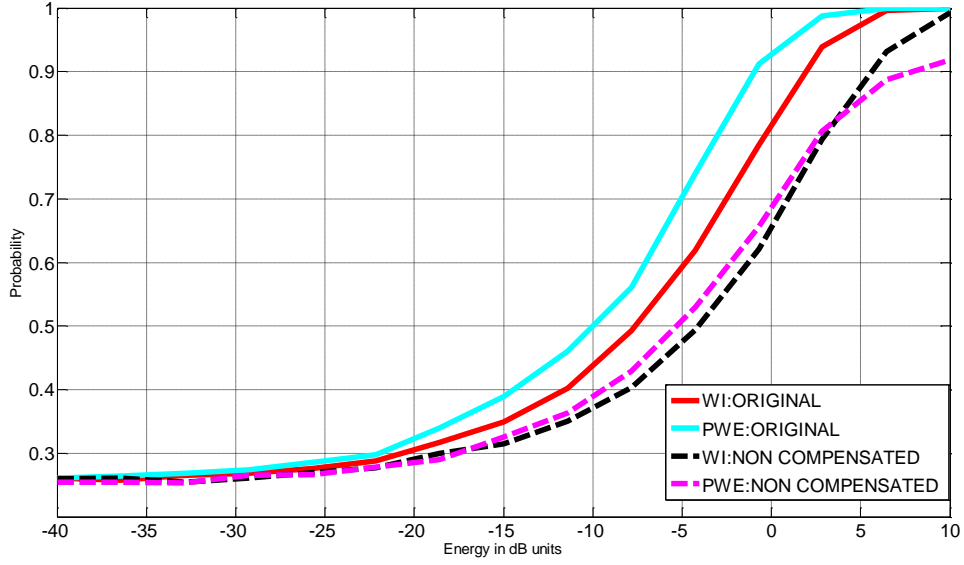


Figure 33. P_{cd} values obtained for “original” wideband, non-compensated wideband, “original” and non-compensated PWE waveforms with 2 transmissions and target moving away from radar.

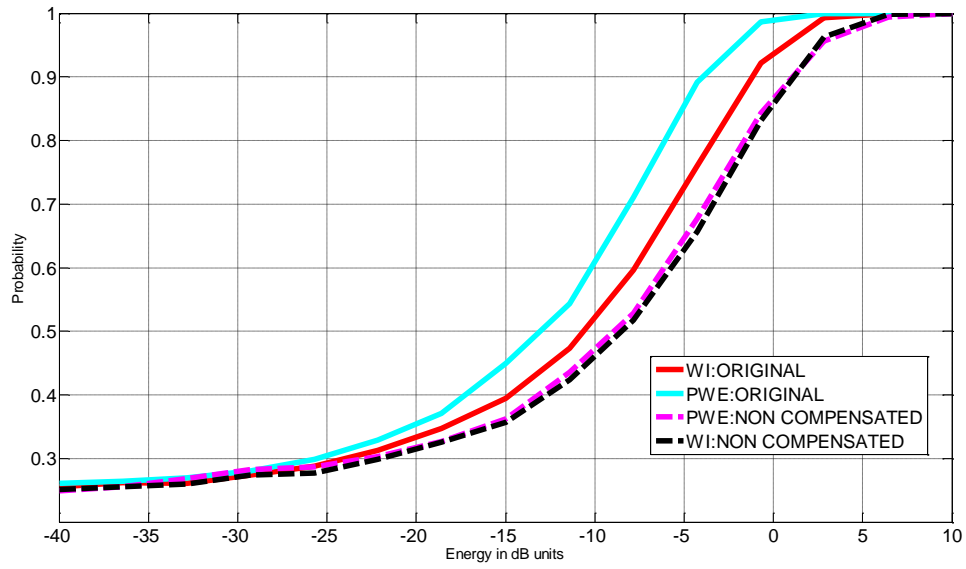


Figure 34. P_{cd} values obtained for “original” wideband, non-compensated wideband, “original” and non-compensated PWE waveforms with 4 transmissions and target moving away from radar.

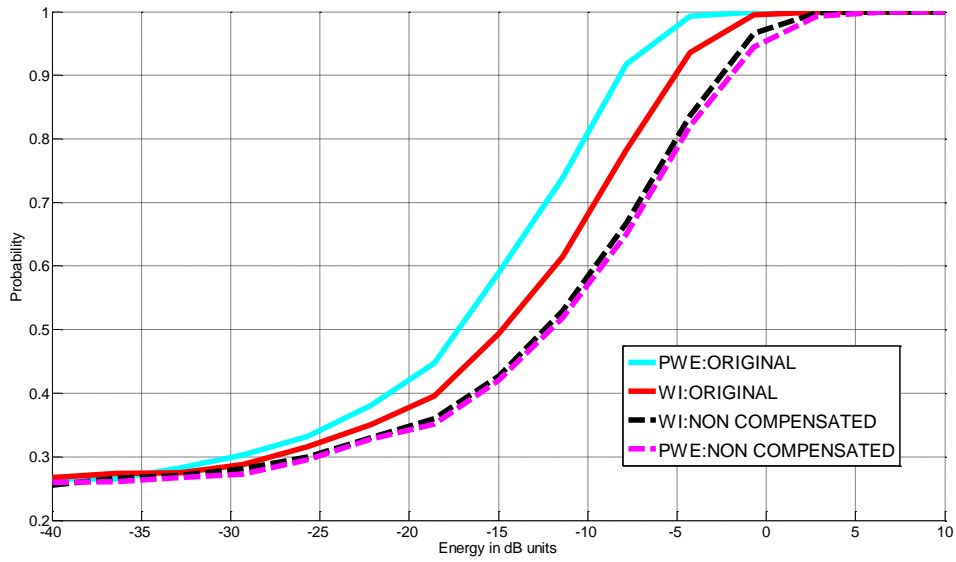


Figure 35. P_{cd} values obtained for “original” wideband, non-compensated wideband, “original” and non-compensated PWE waveforms with 10 transmissions and target moving away from radar.

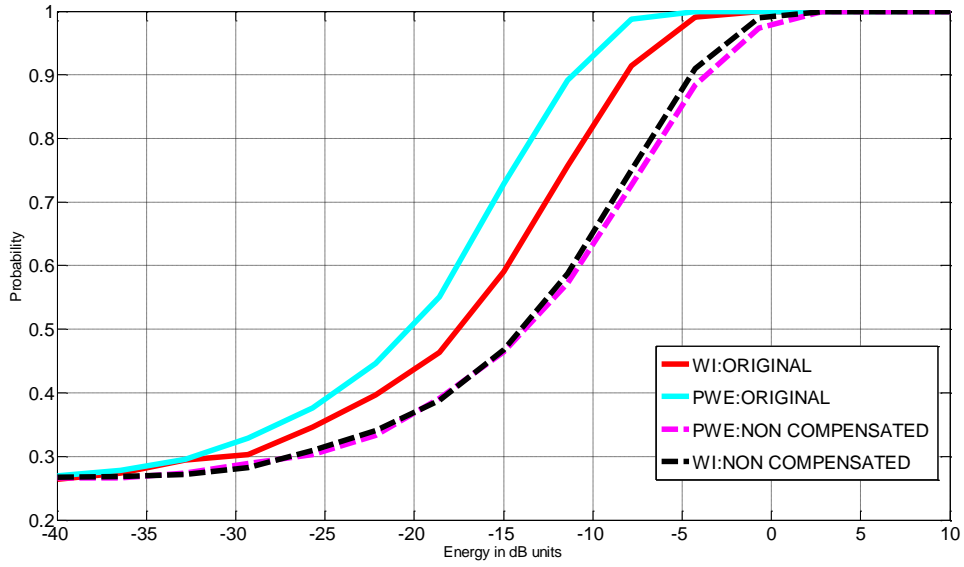


Figure 36. P_{cd} values obtained for “original” wideband, non-compensated wideband, “original” and non-compensated PWE waveforms with 20 transmissions and target moving away from radar.

E. MOTION COMPENSATED WAVEFORMS

1. Introduction

As mentioned in previous section we have two different types of motion. The probability of correct decision (P_{cd}) with different numbers of transmissions for different values of energy is shown in Figure 37 to Figure 53.

2. Decreasing Range between the CR and Target – Wideband Waveform

In this series of Monte Carlo simulations, we use the compensated wideband waveform. Monte Carlo simulations are performed and performance curves are generated for energy values from -40dB to 0dB units.

The performance of the compensated wideband waveform for 10, 20 and 30 transmissions is presented in Figure 37 (illustrated by dashed lines: blue for 10 transmissions, red for 20 transmissions and green for 30 transmissions). As shown in Figure 37, there is a remarkable improvement in P_{cd} as we increase the number of

transmissions. For instance, for -10dB energy units for 10 transmissions P_{cd} is equal to 0.7 (blue dashed curve); for 20 transmissions is equal to 0.87 (red dashed curve) and for 30 transmissions is equal to 0.93 (green dashed line). To achieve a P_{cd} of 0.9 by using a compensated wideband waveform, we need: -5.1dB units for 10 transmissions, -8dB units for 20 transmissions; and only -12dB units for 30 transmissions.

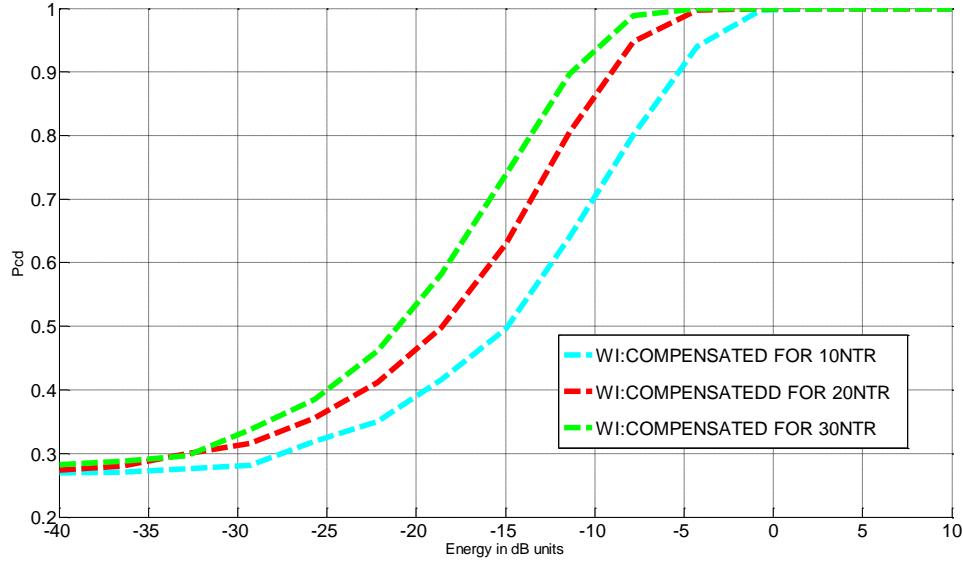


Figure 37. P_{cd} values obtained for compensated wideband waveform with 10, 20 and 30 transmissions and approaching target.

3. Decreasing Range between the CR and Target – Comparison between Compensated and Non-compensated Waveforms

The comparison between the compensated and non-compensated waveforms (wideband and PWE) when the target approaches the static radar (the range is decreasing) is shown in figures 38, 39, 40, and 41. The same energy values are used (-40dB to 10dB units). The performance comparisons using 2, 4, 10 and 20 transmissions are shown in figures 38, 39, 40, and 41 respectively. Looking at these four figures we note several observations. First, in all four cases, PWE compensated waveform (dashed blue line) has superior performance compared to the wideband compensated waveform (dashed red line). The P_{cd} performance improvement given fixed number of transmissions is evident.

For instance, from Figure 38 we observe that in case of -5dB energy level P_{cd} is equal to 0.5 for non-compensated PWE waveform (dashed green line) but for PWE compensated waveform (dashed blue line) P_{cd} is equal to 0.7. The improvement in P_{cd} by using the PWE compensated waveform is slightly different if we increase the number of transmissions. For example, from figures 39, 40 and 41 the performance difference given -5dB units of transmit energy between compensated and non-compensated PWE waveforms is: 0.21 for 4 transmissions, 0.2 for 10 transmissions, and 0.22 for 20 transmissions. Another observation can be made if we use a specific probability threshold. For instance, suppose we set a P_{cd} of 0.9 and suppose we use only 10 transmissions (Figure 40). The energy required according to the plot is: -8dB units for the PWE compensated waveform, -6dB units for the wideband compensated waveform, -3dB units for the non-compensated wideband waveform and, -2dB units for the non-compensated PWE waveform. Thus, we save 6dB units of energy if we use the PWE compensated waveform instead of the non-compensated one if we want to achieve the same P_{cd} . In contrast, the improvement in the case of wideband waveforms is only 3dB energy units. We observe similar results for the other numbers of transmissions. The difference in terms of P_{cd} between the waveforms for 20 transmissions is shown in Figure 41. For the same probability of 0.9 the difference between compensated and non-compensated PWE waveforms is almost 11dB energy units. Between the compensated and non-compensated wideband waveforms the difference is almost 7dB energy units. Finally, for higher number of transmissions with the compensated waveforms, the improvement we achieve in terms of P_{cd} and energy is greater, especially by using the compensated PWE waveform.

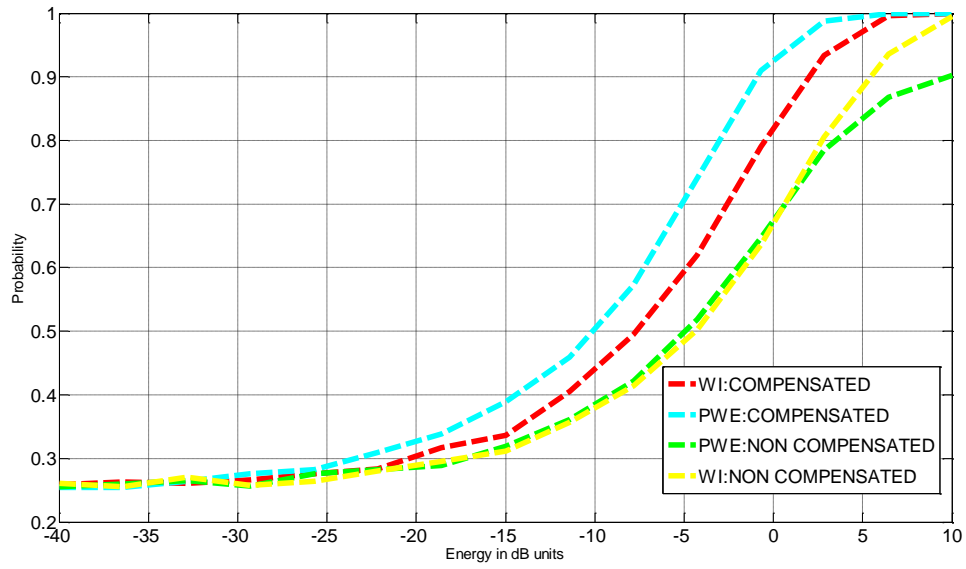


Figure 38. P_{cd} levels obtained for compensated and non-compensated waveforms for 2 transmissions and approaching target.

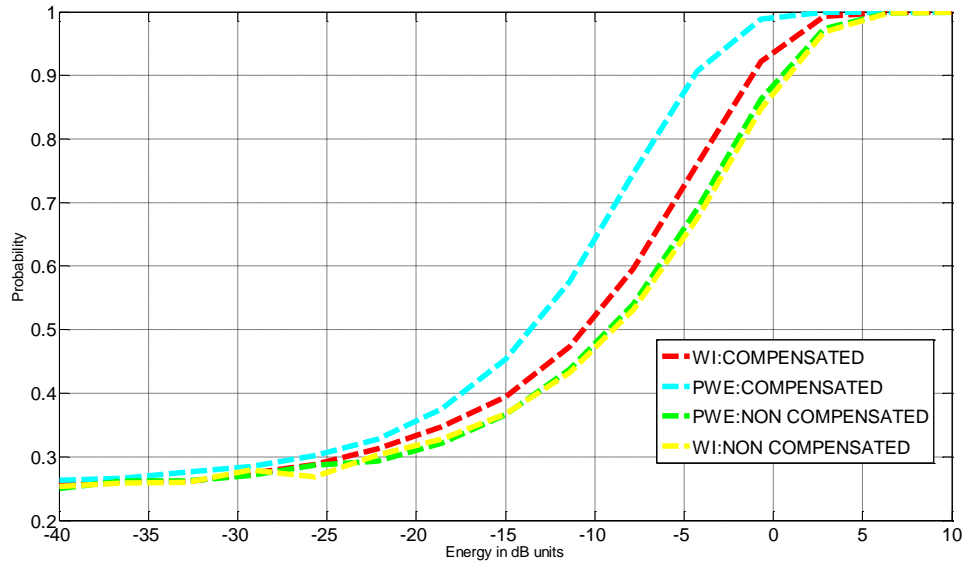


Figure 39. P_{cd} levels obtained for compensated and non-compensated waveforms for 4 transmissions and approaching target.

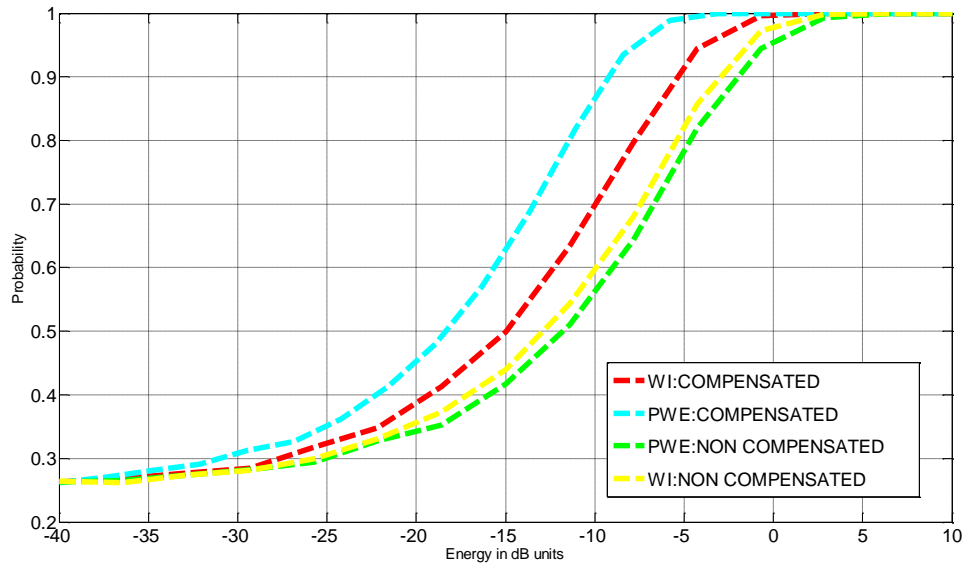


Figure 40. P_{cd} levels obtained for compensated and non-compensated waveforms for 10 transmissions and approaching target.

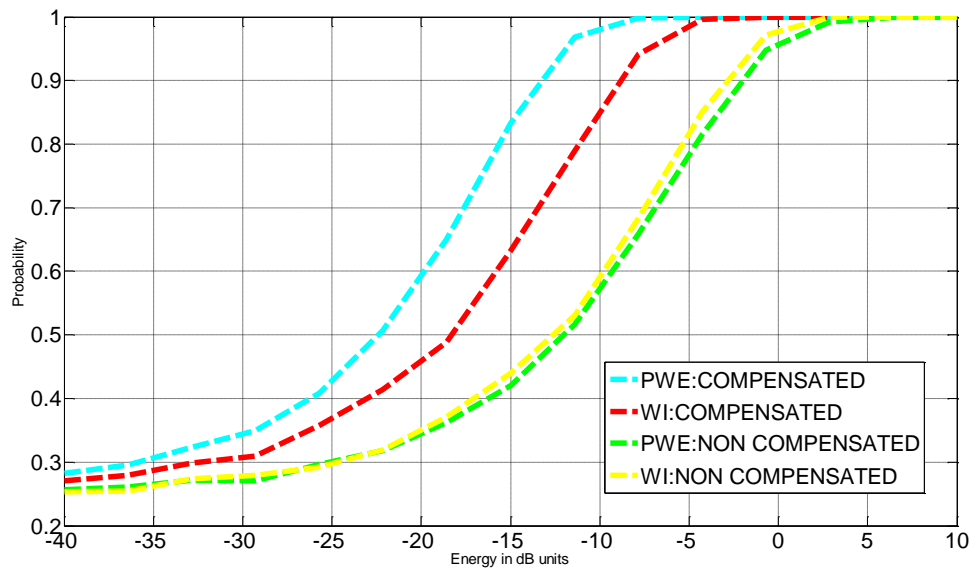


Figure 41. P_{cd} levels obtained for compensated and non-compensated waveforms for 20 transmissions and approaching target.

4. Increasing Range between the CR and Target – Comparison between Compensated and Non-compensated Waveforms

The use of compensated waveforms (wideband and PWE) is shown to be an effective mitigation for target motion (target moving away from the CR). The comparison in terms of P_{cd} between the compensated and non-compensated wideband and PWE waveforms is shown by figures 42, 43, 44 and 45. As depicted in these figures, the waveform with the superior performance in all cases of number of transmissions (2, 4, 10 and 20 transmissions) is the compensated PWE waveform (dashed blue line). Moreover, for low energy values the improvement in terms of P_{cd} for PWE and wideband waveform is moderate. In contrast, for higher energy levels the improvement is clearly remarkable. For instance, in Figure 44 when 10 transmissions are used with an energy level of -10dB units, the improvement in the P_{cd} is equal to 0.18 for the PWE waveform and only 0.01 for the wideband waveform. Furthermore, the use of compensated waveforms results in obvious energy savings both in the case of wideband and PWE waveforms regardless the number of pulsed transmissions. For instance, when we use only two transmissions (Figure 42) and for a probability of 0.9, we need -2dB energy units for the compensated PWE waveform and for the non-compensated PWE waveform 8dB energy units are needed. Thus, this is a difference of 10dB energy units. In the case of wideband waveforms, the difference between the compensated and non-compensated wideband waveform is only 4dB energy units. Another conclusion deduced from figures 42 to 45 is that as we increase the number of transmissions the difference in energy used to achieve a specific P_{cd} is slightly decreased. For instance, for P_{cd} equal to 0.9 the difference between compensated and non-compensated PWE waveforms starts at: 8dB energy units for 2 transmissions, 5dB energy units for 4 transmissions, 4dB energy units for 10 transmissions and 10dB energy units for 20 transmissions.

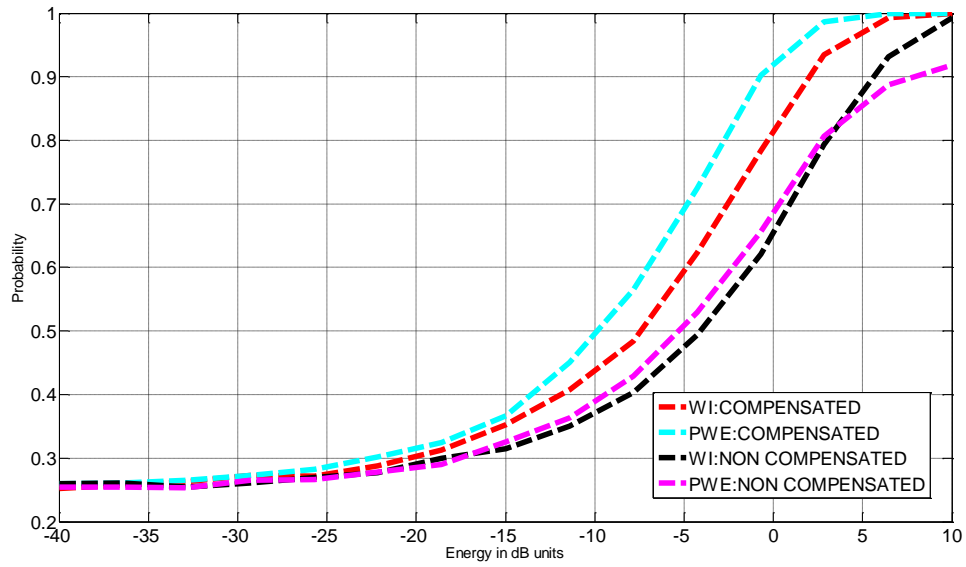


Figure 42. P_{cd} values obtained for compensated and non-compensated waveforms with 2 transmissions and target moving away from radar.

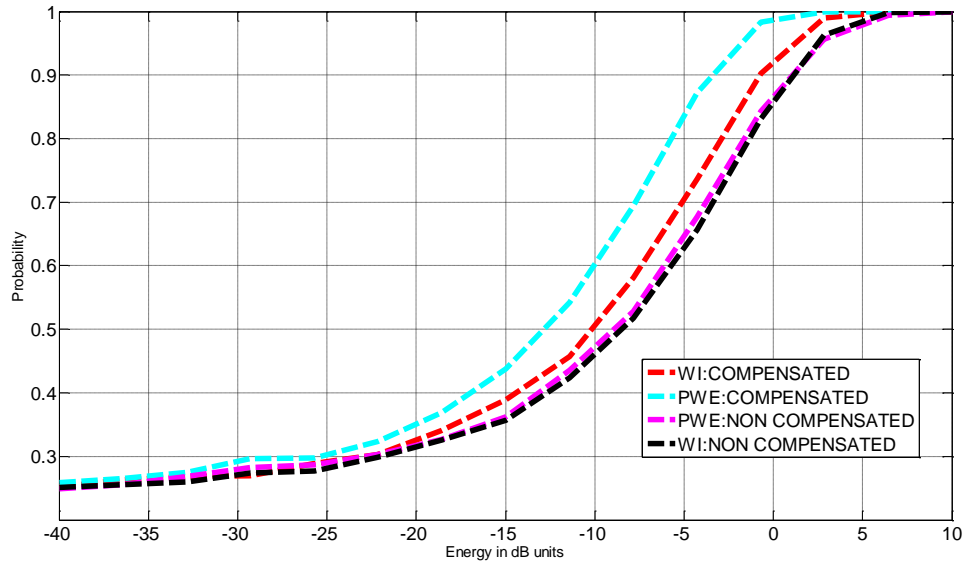


Figure 43. P_{cd} values obtained for compensated and non-compensated waveforms with 4 transmissions and target moving away from radar.

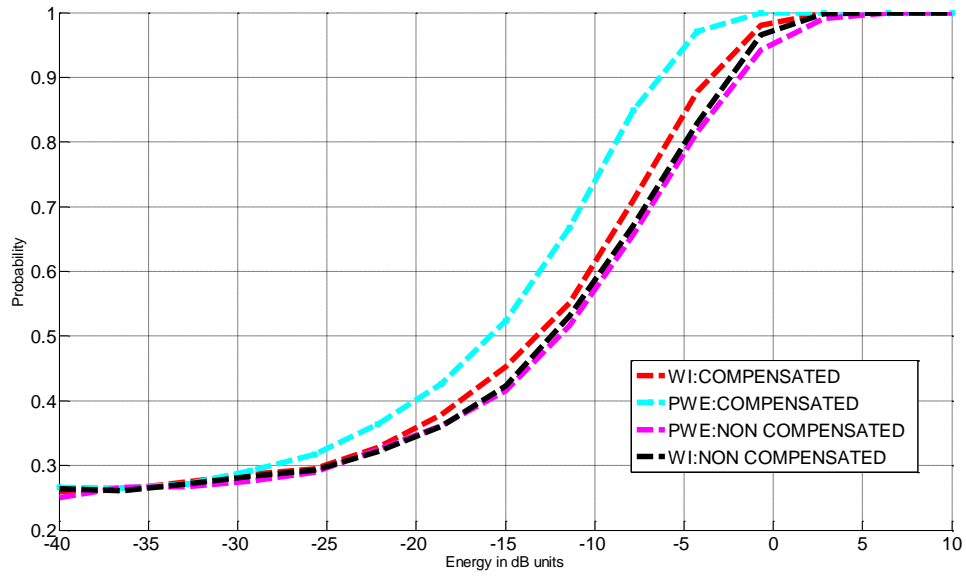


Figure 44. P_{cd} values obtained for compensated and non-compensated waveforms with 10 transmissions and target moving away from radar.

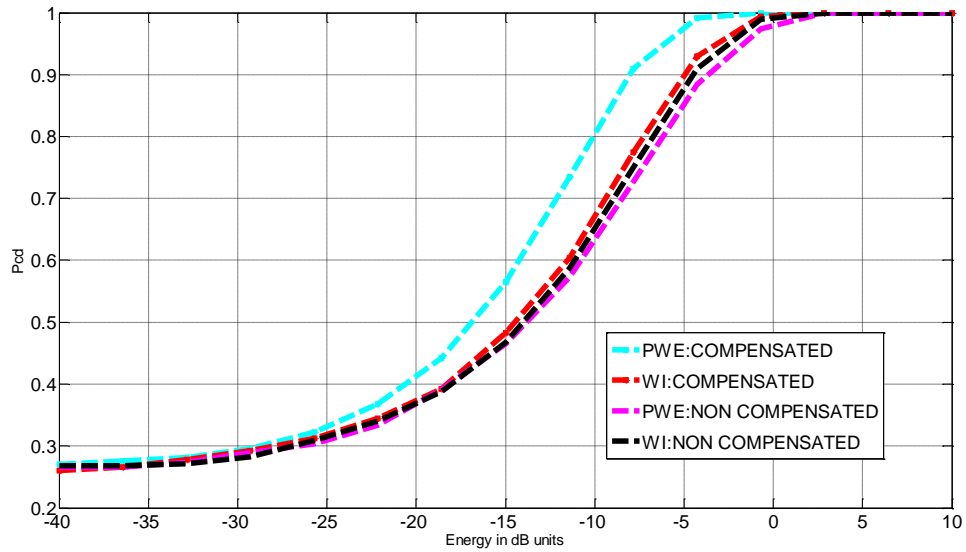


Figure 45. P_{cd} values obtained for compensated and non-compensated waveforms with 20 transmissions and target moving away from radar.

5. P_{cd} for Decreasing Range – Comparison between Original and Compensated Waveforms

The P_{cd} obtained for a specific number of transmissions (in this case, 2, 4, 10, and 20) when the range between radar and the target is decreasing is shown in Figure 46 to Figure 49. In these figures we plot the P_{cd} performance of the “original” wideband waveform, the compensated wideband waveform, the “original” PWE waveform and the compensated PWE waveform for five specific numbers of transmissions. Solid lines correspond to the performance of “original” wideband and PWE waveforms (red and blue color, respectively), and dashed lines correspond to the performance of compensated wideband and PWE waveforms. Recall that the performance labeled “original” actually refers to the case of both static target and radar. Here, we only use it as reference curve.

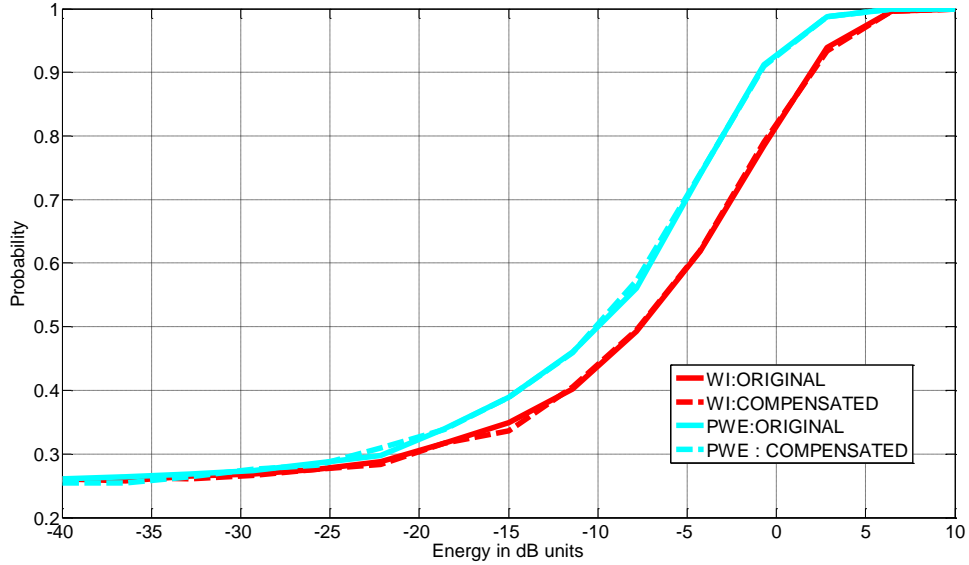


Figure 46. P_{cd} values obtained for “original” wideband, compensated wideband, “original” PWE and compensated PWE waveforms for 2 transmissions and approaching target.

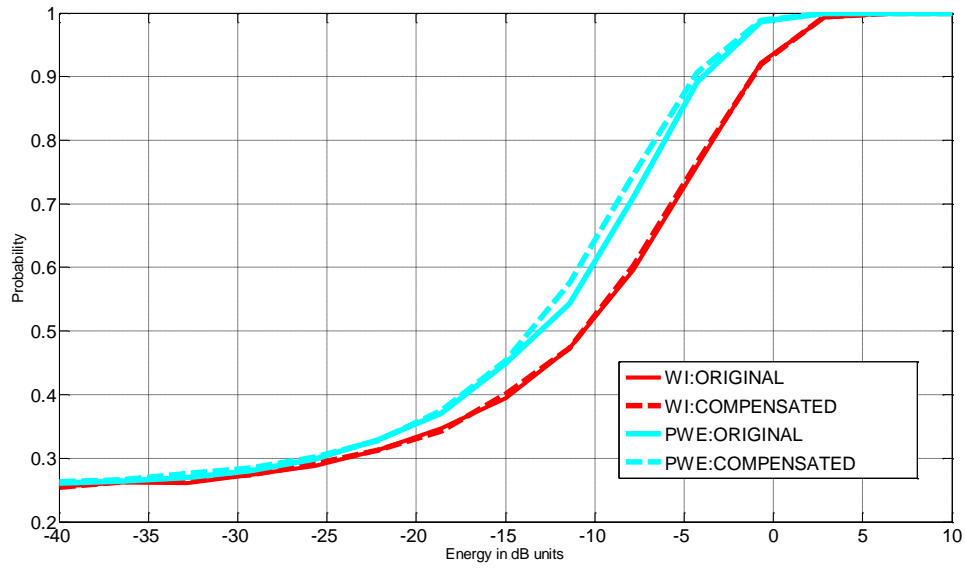


Figure 47. P_{cd} values obtained for “original” wideband, compensated wideband, “original” PWE and compensated waveforms PWE for 4 transmissions and approaching target.

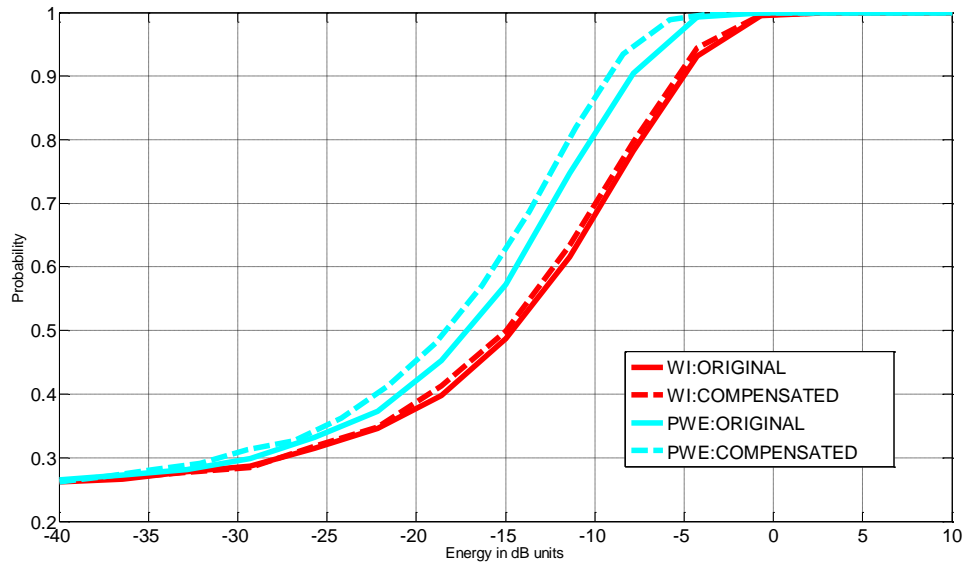


Figure 48. P_{cd} values obtained for “original” wideband, compensated wideband, “original” PWE and compensated PWE waveforms for 10 transmissions and approaching target.

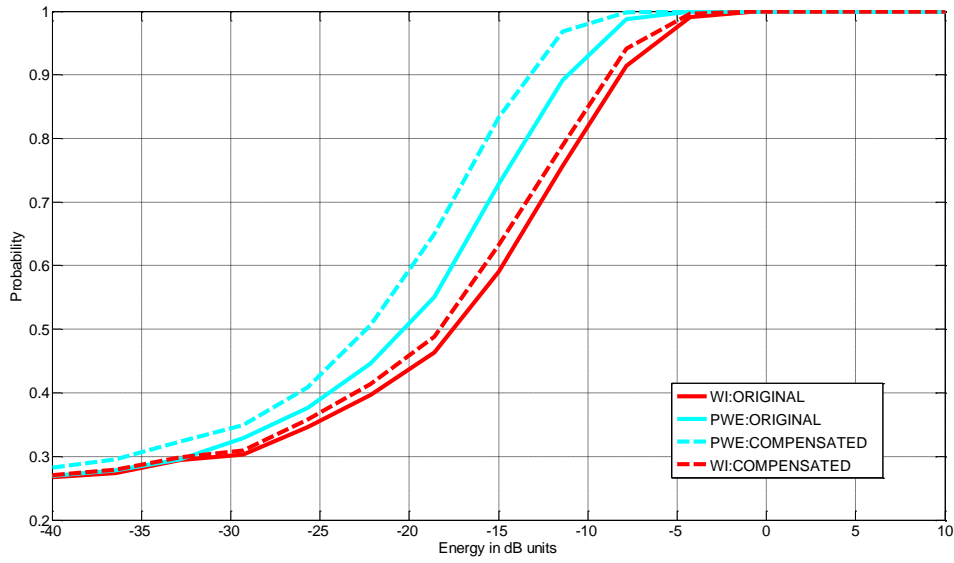


Figure 49. P_{cd} values obtained for “original” wideband, compensated wideband, “original” PWE and compensated PWE waveforms for 20 transmissions and approaching target.

6. P_{cd} for Increasing Range – Comparison between Original and Compensated Waveform

The P_{cd} levels obtained for a specific number of transmissions (2, 4, 10, and 20) when the range between radar and the target is increasing is shown in Figure 50 to Figure 53. Recall again that the performance called “original” actually refers to the case of both static target and radar. We only use it as reference curve.

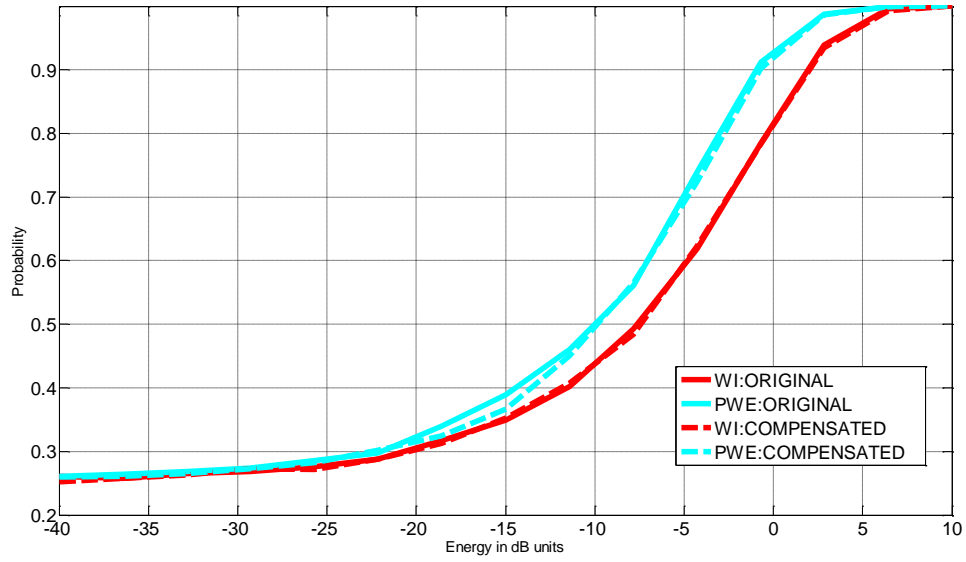


Figure 50. P_{cd} values obtained for “original” wideband, “original” PWE, compensated wideband and compensated PWE waveforms with 2 transmissions and target moving away from radar.

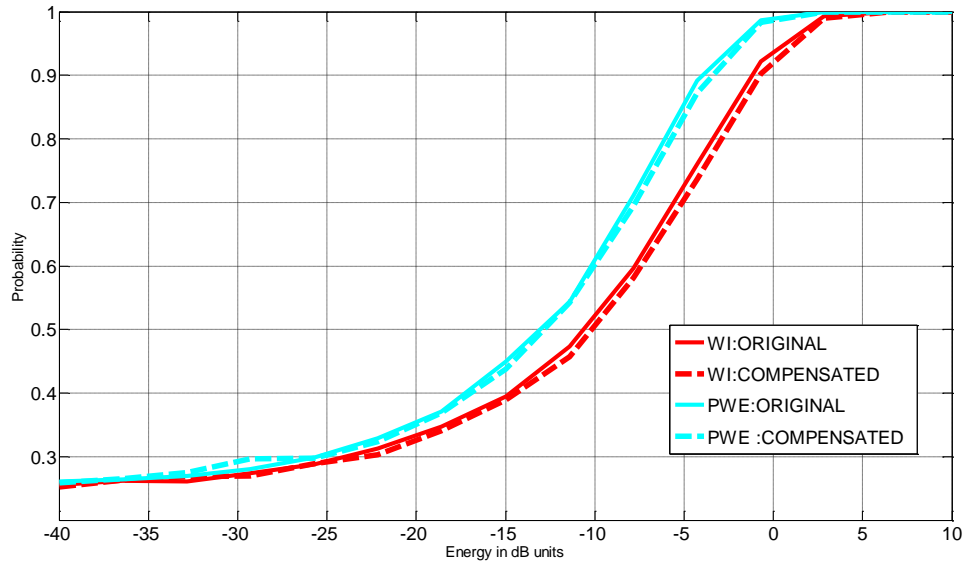


Figure 51. P_{cd} values obtained for “original” wideband, “original” PWE, compensated wideband and compensated PWE waveforms with 4 transmissions and target moving away from radar.

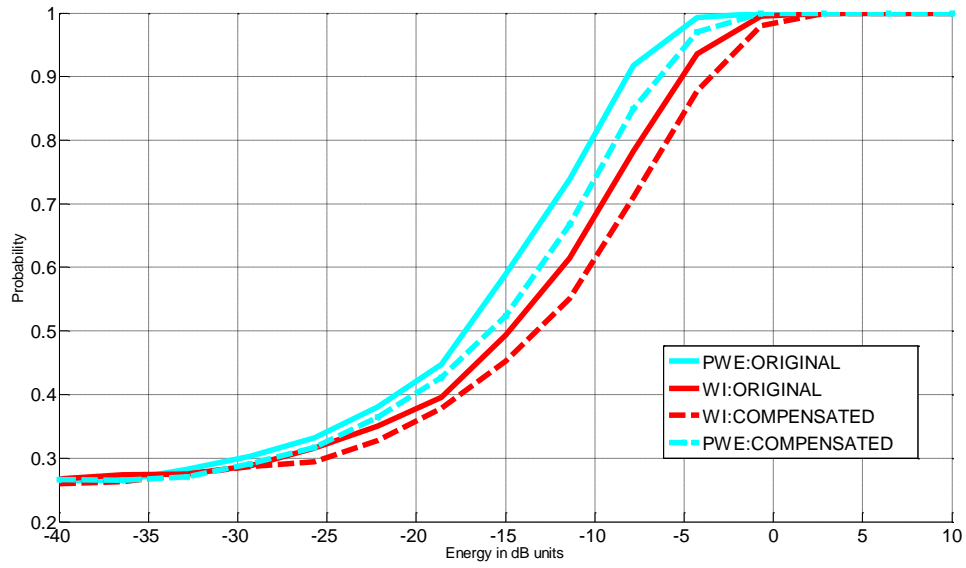


Figure 52. P_{cd} values obtained for “original” wideband, “original” PWE, compensated wideband and compensated PWE waveforms with 10 transmissions and target moving away from radar.

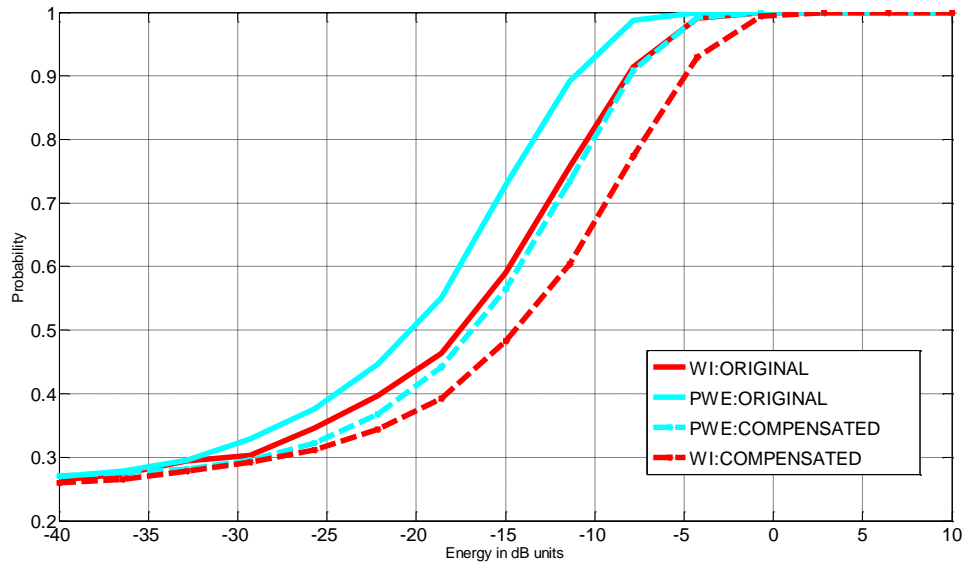


Figure 53. P_{cd} values obtained for “original” wideband, “original” PWE, compensated wideband and compensated PWE waveforms with 20 transmissions and target moving away from radar.

F. CHAPTER SUMMARY

This chapter presented modification to the wideband and PWE waveforms in the case of a static CR system and moving target. We used Monte Carlo simulations to yield the performance plots in order to compare wideband and PWE waveform for different number of transmissions. We drew several conclusions both in the cases of decreasing and increasing distance between the CR and target.

The superior performance of the compensated PWE waveform compared to all the other used waveforms is evident when a target approaches the radar. Even for a small number of transmissions (two and four transmissions) the PWE compensated waveform provides significant improvement in P_{cd} values over the non-compensated waveform. In general, an increase in the number of transmissions improves the P_{cd} regardless of which waveform is used. In our experiments performance improvement is much more apparent for a high number of transmissions such as 10 and 20 transmissions. It is noted that the difference in P_{cd} between the compensated PWE waveform and the non-compensated PWE waveform is much greater than the improvement between the compensated wideband and the non-compensated wideband waveform. This result proves the effectiveness of the PWE waveform over the wideband waveform. We also explored the case when target moves away from the radar. Again, the compensated PWE waveform and the compensated wideband waveform performed better than the uncompensated waveforms. In general, when the number of transmissions is increased the P_{cd} level is increased for all waveforms used. However, in all cases the best performance is seen with the PWE compensated waveform.

It should be noted that regardless of the number of transmissions, low energy values (less than -20dB units) result in P_{cd} of about 0.25 as expected. Thus, the waveform design does not improve the radar performance when low energy levels are used. In contrast, for higher values of energy the improvement of the radar's P_{cd} performance is remarkable. The increase in the number of transmissions results in P_{cd} improvement, especially when the compensated PWE waveform is used. Although CR

also improves the P_{cd} in the case of the wideband waveform, the PWE waveform is more effective. Practically speaking, this means that by using PWE waveform we improve radar's performance. This is critical in real life radar operations. Using the compensated version of wideband and PWE waveforms we achieve better P_{cd} performance using less energy in both cases of target movement (approaching or moving away from the radar).

THIS PAGE INTENTIONALLY LEFT BLANK

V. CONCLUSIONS AND RECOMMENDATIONS

The basic characteristics of cognitive radar (CR) were briefly discussed in this thesis [9]. We used the specific form of CR introduced in [6] for target recognition. Moreover, the probability weighted energy (PWE) waveform (in [7]) is used in our experiment.

Two different methods of using a CR system were discussed. The performance metrics ACTP, ANTR, ApNTCD and MTNCD were investigated. The first method used a probability threshold (for instance, 0.95 or higher) without limiting the number of pulsed transmissions and the second one used a fixed number of transmissions. From the results produced via Monte Carlo simulations, we deduced that relatively high energy a specific probability threshold without restraining the pulsed transmissions must be used in order to keep radar's performance in satisfactory level in terms of P_{cd} (first method of using a target recognition CR). In contrast, if the available energy is low, it is better to use for a specific number of transmissions (second method of using a target recognition CR).

In the latter part of the thesis, the case of a static target recognition CR and moving extended target was introduced. Furthermore, the changes in time and amplitude for a target moving away or approaching the CR system was discussed. In our simulation we had to account for these changes. The performance of wideband and PWE waveforms with different values of energy for different numbers of transmissions was compared. Furthermore, a general conclusion is made that if the target response changes but the waveform design is not modified the P_{cd} drastically decreases. In order to compensate radar's performance two modified types of waveforms were used: the compensated wideband waveform and the compensated PWE waveform. From the comparison between the compensated and uncompensated waveforms, P_{cd} improvement was shown when different values of energy for different numbers of pulsed transmissions were used. With target motion, the PWE compensated waveform had the best performance as compared to other waveforms even when small energy values were used. Different

configurations of moving CR systems and targets should be included in a future investigation.

LIST OF REFERENCES

- [1] M. R. Bell, "Information Theory and radar waveform design," *IEEE Trans. Inform. Theory*, vol. 39, no. 5, pp. 1578–1597, Sep. 1993.
- [2] S. U. Pillai, H. S. Oh, D. C. Youla and J. R. Guerci, "Optimum transmit-Receiver design in the presence of signal-dependent interference and channel noise," *IEEE Trans. Inform. Theory*, vol. 46, no. 2, pp. 577–584, Mar. 2000.
- [3] R. Romero, J. Bae and N. Goodman, "Theory and Application of SNR and Mutula Information Matched Illumination Waveforms," *Aerospace and Electronic Systems*, IEEE, vol. 47, no. 2, pp. 912–927, Apr. 2011.
- [4] R. Romero and N. Goodman, "Information-theoretic matched waveform in signal dependent interference," in (RADAR'08), *Proceedings of the 2008 IEEE Radar Conference*, Rome, Italy, May 26–30, 2008.
- [5] S. Kay, "Optimal signal design for detection of Gaussian point targets in stationary Gaussian clutter/reverberation," *IEEE J. Sel. Topics in Sig. Proc. Mag*, vol. 1, no. 1, pp. 31–41, 2007.
- [6] N. Goodman, P. Venkata and M. Neifeld, "Adaptive waveform design and sequential hypothesis testing for target recognition with active sensors," *IEEE J. Sel Topics in Sig. Proc. Mag*, vol. 1, no. 1, pp. 105–113, 2007.
- [7] R. Romero and N. Goodman, "Improved waveform Design for Target Recognition with Multiple Transmissions," in *Waveform Diversity and Design Conference*, 2009 International, Orlando, FL, Feb 8–13, 2009.
- [8] R. A. Romero, "Detection Performance of Matched Transmit Waveform for Moving Extended Targets," submitted to *2013 Asilomar Conference on Signal, Systems and Computers*, Nov. 2013.
- [9] S. Haykin, "Cognitive Radar.A way of the future," *IEEE Signal Processing Magazine*, vol. 23, no. 1, pp. 33–40, Jan. 2006.
- [10] M. G. Bruno and J. M. Moura, "Multiframe detector/tracker: Optimal perfomance," *IEEE Trans. Aerosp. Electron. Syst.*, vol. 37, pp. 925–944, Jul. 2001.

- [11] R. Bakker, T. Kirubarajan, B. Currie and S. Haykin, "Adaptive radar detection: A bayesian approach," in *Proc. EPSRC IEE Workshop Nonlinear Non-Gaussian Signal Processing*, Peebles, Scotland, Jul. 2002.
- [12] N. A. Goodman, "Closed-Loop Radar with Adaptively Matched Waveforms," in *Electromagnetics in Advanced Applications*, 2007, ICEAA 2007, Torino, Italy, 17–21 Sep. 2007.

INITIAL DISTRIBUTION LIST

1. Defense Technical Information Center
Ft. Belvoir, Virginia
2. Dudley Knox Library
Naval Postgraduate School
Monterey, California